Polymer 50 (2009) 5–32

Contents lists available at ScienceDirect

Polymer

journal homepage: www.elsevier.com/locate/polymer

Feature Article

Core cross-linked star polymers via controlled radical polymerisation

Anton Blencowe, Jing Fung Tan, Tor Kit Goh, Greg G. Qiao*

Polymer Science Group, Department of Chemical and Biomolecular Engineering, The University of Melbourne, Melbourne 3010, Australia

ARTICLE INFO

Article history:
Received 3 June 2008
Received in revised form
30 September 2008
Accepted 30 September 2008
Available online 4 October 2008

Keywords:
Star polymer
CCS
Controlled radical polymerisation
Arm-first
Macroinitiator
Macromonomer
Cross-linker
Miktoarm
ATRP
NMP
RAFT
Copolymer
Morphology
Catalysis
Encapsulation
Polymer therapeutics
Honeycomb
Polyelectrolytes

ABSTRACT

Star polymers are comprised of multiple arms or branches radiating from a central point or core and have been of huge scientific interest since they were first prepared sixty years ago, as a result of their unique physical properties. Star polymers are not just an academic curiosity, but are currently employed or under investigation in a wide range of industries and commercial materials ranging from engine oils and coating technologies to contact lenses and biomedical devices. Although there are many different types of star polymers and methods for their synthesis, recent advances in the field of controlled radical polymerisation have enabled the facile production of complex star polymer architectures from a large range of monomer families, without the requirement of highly stringent reaction conditions. In particular, well-defined, nanometre scale core cross-linked star (CCS) polymers, which are readily accessible by controlled radical polymerisation techniques, have been increasingly prominent in the scientific literature. As a result, this feature article provides a comprehensive review covering the development, functionalisation, physical properties and application of core cross-linked star polymers prepared by controlled radical polymerisation and the arm-first approach.

1. Introduction

The development of controlled polymerisation techniques initiated by the seminal studies of Szwarc [1] has enabled polymer scientists to prepare a wide variety of complex macromolecular architectures with well-defined molecular weights, structural and compositional homogeneity [2]. In particular, star polymers with three-dimensional (3D) globular structures have long been studied for their unique properties, which facilitate their application to advanced materials. The preparation of star polymers via controlled polymerisation techniques can be divided into three general synthetic methods: (i) The 'core-first' approach ('from-approach'), in which a multifunctional initiator is employed to simultaneously initiate the polymerisation of vinylic monomers, thus forming the arms of the star polymer (Scheme 1a). (ii) The 'arm-first' approach involves the reaction of a living macroinitiator (MI) (or macromonomer (MM)), the arm, with a difunctional (or higher) vinylic cross-linker to form a densely cross-linked core from which the arms radiate (Scheme 1b). Whereas the cross-linking of MMs or preformed micelles with core isolated vinyl groups can be regarded as a 'through-approach', the cross-linking of MIs with cross-linkers is complicated by the fact that multiple mechanisms can occur simultaneously (*vide infra*). For example, the cross-linking of block copolymers with pendent vinyl groups (formed from the reaction of MIs with cross-linkers) can be considered as a 'through-approach', whereas the attack of an active MI with the pendent vinyl groups on a preformed star could be regarded as a 'to-approach'. Thus the formation of star polymers from MIs and cross-linkers is a combination of both to- and through-approaches. (iii) The third method, namely the 'grafting to-approach', can be considered as a combination of controlled polymerisation and coupling reactions; initially, a well-defined polymer, the arm, is prepared via controlled

* Corresponding author. Tel.: +61 383 448665; fax: +61 383 444153.
E-mail address: gregghq@unimelb.edu.au (G.G. Qiao).

0032-3861/$ – see front matter © 2008 Elsevier Ltd. All rights reserved.
doi:10.1016/j.polymer.2008.09.049

Symbols and abbreviations

3D	three-dimensional
η_0	zero-shear viscosity
ϕ_{eff}	effective volume fraction
α	activity coefficient
AA	acrylic acid
AIBN	2,2′-azobis(2-methylpropionitrile)
AFM	atomic force microscopy
ATRP	atom transfer radical polymerisation
$ATRP_{(Cu)}$	copper mediated ATRP
$ATRP_{(Ru)}$	ruthenium mediated ATRP
n-BA	*n*-butyl acrylate
BAM	bisphenol A dimethacrylate
BDDA	1,4-butandiol diacrylate
n-BMA	*n*-butyl methacrylate
BMI	1,1′-(methylenedi-4,1-phenylene)bismaleimide
bpy	2,2′-bipyridine
t-BSt	4-*t*-butylstyrene
CCS	core cross-linked star
CRP	controlled radical polymerisation
D_0	measured nearest-neighbour distance
$D(c)$	translational diffusion coefficient
D_h	hydrodynamic diameter
DLS	dynamic light scattering
DMAP	4-(*N*,*N*-dimethylamino)pyridine
DOTA	1,4,7,10-tetraazacyclododecanetetraacetic acid
DP	degrees of polymerisation
DVB	divinylbenzene
EGDA	ethylene glycol diacrylate
EGDMA	ethylene glycol dimethacrylate
f	number of arms
FT-IR	Fourier transform infrared
G'	storage modulus
G''	loss modulus
GTP	group transfer polymerisation
GPC	gel permeation chromatography
HDA	1,6-hexanediol diacrylate
HEA	poly(2-hydroxyethyl acrylate)
IDA	isotopic dilution assay
LA	lactic acid
LCST	lower critical solution temperature
$m_{(AG)}$	mass contribution of the additional core-incorporated group
$m_{(CL)}$	mass contribution of the cross-linker
MA	methyl acrylate
MALLS	multi-angle laser light scattering
MAO	methylaluminoxane
MI	macroinitiator
MM	macromonomer
Mol. $wt._{(CL)}$	molecular weight of the cross-linker
Mol. $wt._{(AG)}$	molecular weight of the additional core-incorporated group
M_n	number-average molecular weight
M_p	peak molecular weight
MPS	mononuclear phagocytic system
M_w	weight-average molecular weight
$M_{w(arm)}$	arm weight-average molecular weight
$M_{w(CC)}$	M_w values determined using a conventional calibration with linear standards
$M_{w(CCS)}$	CCS polymer weight-average molecular weight
$M_{w(MALLS)}$	M_w values determined using multi-angle laser light scattering
$M_{w(MI)}$	MI weight-average molecular weight
$M_{w(UC)}$	M_w values determined using a universal calibration with a triple detector system
NAS	*N*-acryloxysuccinimide
NMP	nitroxide mediated polymerisation
PAA	poly(acrylic acid)
PAH	poly(allylamine hydrochloride)
P^nBA	poly(*n*-butyl acrylate)
P^tBA	poly(*t*-butyl acrylate)
P^nBMA	poly(*n*-butyl methacrylate)
P^tBSt	poly(4-*t*-butylstyrene)
PDI	polydispersity index
PDMA	poly(*N*,*N*-dimethylacrylamide)
PE	polyethylene
PEG	poly(ethylene oxide)
PEGDMA	poly(ethylene glycol dimethacrylate)
PEGMA	poly(ethylene glycol) methacrylate
PET	positron emission topography
PMDETA	*N*,*N*,*N*′,*N*″,*N*″-pentamethyldiethylenetriamine
PMMA	poly(methyl methacrylate)
PNIPAM	poly(*N*-isopropylacrylamide)
PSt	polystyrene
PTSA	*p*-toluenesulfonic acid
q	scattering vector
QCM	quartz crystal microbalance
RAFT	reversible addition–fragmentation chain transfer
R_c	core radius
R_g	radius of gyration
R_h	hydrodynamic radius
R_p	CCS polymer radius
ROMP	ring-opening metathesis polymerisation
ROP	ring-opening polymerisation
(*R*,*S*)-BINOL	racemic mixture of 1,1′-bi(2-naphthol)
SANS	small-angle neutron scattering
SAXS	small-angle X-ray scattering
SEM	scanning electron microscopy
SH	cleaved bis(2-methacryloyloxyethyl)disulfide
SLS	static light scattering
SS	bis(2-methacryloyloxyethyl)disulfide
T^iBA	triisobutylaluminium
TEM	transmission electron microscopy
TEMPO	2,2,6,6-tetramethylpiperidine-1-oxyl
T_g	glass transition temperature
TMA	trimethylaluminium
TMS	trimethylsilane
4VBA	4-vinylbenzoic acid
4VP	4-vinylpyridine
2VP	2-vinylpyridine
$WF_{(arms)}$	weight fraction of arms in the CCS polymer
$X_{(CL)}$	fractional conversion of cross-linker
$X_{(MI)}$	fractional conversion of MI to CCS polymer

polymerisation and coupled to a multifunctional linking agent that acts as the core (Scheme 1c). However, it should be noted that for arms prepared by controlled radical polymerisation (CRP) it is generally necessary to appropriately modify the active terminal group to enable coupling with the multifunctional linking agent.

Although the three synthetic methods mentioned above are all well established and can be conducted using a variety of controlled polymerisation techniques, they have various advantages and disadvantages, which make them suited to the preparation of particular types of stars. For example, the core-first approach

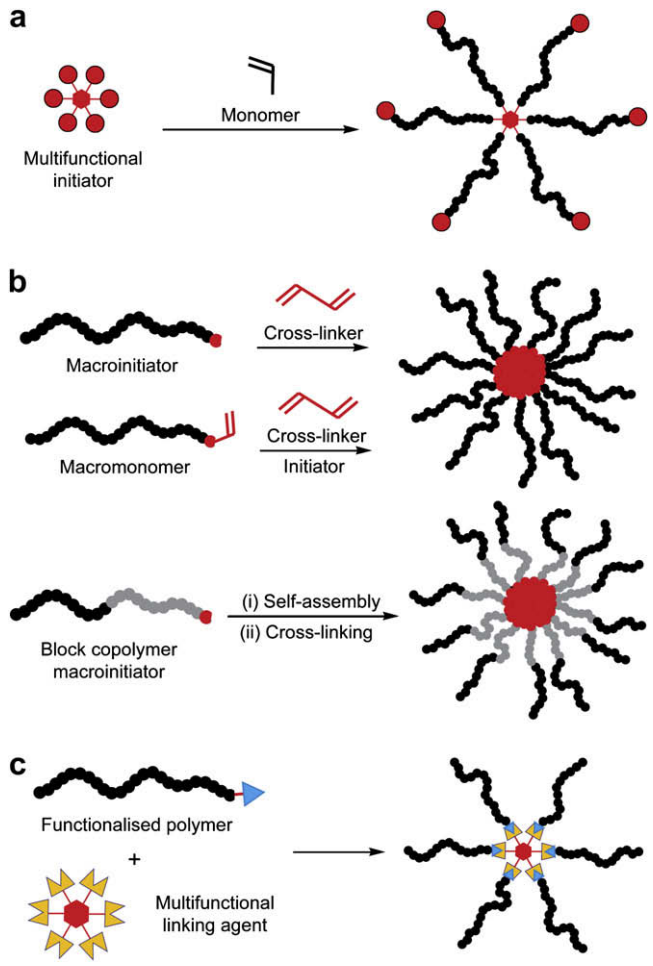

Scheme 1. Synthetic approaches for the preparation of star polymers via controlled polymerisation techniques; (a) the core-first approach, (b) the arm-first approach and (c) grafting to-approach.

allows for the preparation of well-defined star polymers with a precise number of arms, which can be controlled by the number of initiating functions present on the multifunctional initiator, provided that the initiating sites are of equal reactivity and the rate of initiation is higher than the rate of propagation. Perhaps the most beneficial aspects of this approach are the very high yields and the ease with which the pure star polymer can be isolated, given that the crude reaction mixture only requires separation of any unreacted monomers. However, this approach is not well-suited to the preparation of miktoarm stars unless specially designed multifunctional initiators with orthogonal initiating functions are employed. Similarly, the preparation of stars with high arm number (>30) requires the synthesis of complex and highly functionalised initiators. Furthermore, the molecular weight of the arms cannot be measured directly, although the number of arms can be indirectly determined via several methods, including end-group analysis, determination of branching parameters and isolation of the arms after cleavage. Another drawback that applies when CRP methods are employed for the core-first approach is the need for special precautions to prevent star–star coupling. In comparison, it is significantly more difficult to obtain well-defined stars via the arm-first approach even though the degree of polymerisation (DP) of the arms can be well-controlled as they are synthesised independently, the number of arms incorporated into the stars is influenced by many parameters and the stars invariably possess broad arm number distributions. In addition, incomplete conversion of the MI or MM to star leads to the need for lengthy fractional precipitation or dialysis protocols. However, the arm-first approach is unique in that you can produce stars with very large numbers of arms (>100) with relative ease and the stars possess a significantly sized cross-linked core (relative to the overall molecular weight of the macromolecule) into which functionality can be readily incorporated. These large cores have a high capacity that renders this type of star ideal for site specific isolation. The arm-first approach also enables the facile preparation of miktoarm stars via both the 'in–out' and the 'multi-macroinitiator' methods (*vide infra*). The grafting to-approach for the preparation of stars offers the greatest degree of control over the final macromolecular architecture as both the synthesis of the arms and the core can be conducted in a very precise manner, and the number of arms is controlled by the functionality of the multifunctional linking agent provided that the coupling reaction is quantitative. However, very long reaction times and an excess of arms are often required to obtain quantitative conversion, leading to need for lengthy purification procedures. Furthermore, it is exceedingly difficult to produce stars with a large number of arms (>20) as steric congestion about the core hinders the coupling reaction and leads to incomplete grafting even at very long reaction times. Like the arm-first approach, the grafting to-approach provides a facile way to prepare miktoarm stars through the application of several chemically different arms with identical and complementary functionality through which it can couple to the multifunctional linking agent. All of the approaches discussed are capable of yielding peripheral, arm and core functionalised stars, although the arm-first approach stands-out for its ability to afford stars with large, highly functionalised cores with unique micro-environments generated by their cross-linked nature.

Although the star polymers prepared via the aforementioned methods adopt similar globular or spherical conformations dependent on the arm size, number and composition, it is evident that the core structures are considerably different. Whereas star polymers prepared using multifunctional coupling agents and discrete multifunctional initiators possess cores of negligible molecular weight relative to the macromolecule, star polymers prepared by the arm-first approach have cores which typically account for 10–30% of the polymers' molecular weight. A further distinguishing feature of star polymers prepared via the arm-first approach is the densely cross-linked structure of the core, which lacks the mobility associated with hyperbranched cores present in star polymers prepared from hyperbranched or dendritic multifunctional initiators via the core-first approach. Thus, it seems necessary to disambiguate star polymers prepared via the arm-first approach from other star polymers. Therefore, this class of star polymer will be referred to as 'core cross-linked star (CCS) polymers' as this term better represents the macromolecular architecture, although, in the literature they have also been referred to as star polymers, star microgels, star-like microgels, star nanogels, core–shell stars, nanoparticles and core cross-linked micelles. In addition to this classification, it is also possible to divide CCS polymers into two further sub-categories, namely symmetrical and asymmetrical. Whereas symmetrical CCS polymers are comprised of identical arms, asymmetry is introduced when arms of different molecular weights, chemical compositions or topologies are incorporated into the same macromolecule.

The successful preparation of CCS polymers was first reported by Zilliox et al. in 1968 [3] and involved the anionic polymerisation of living polystyrene (PSt) with divinylbenzene (DVB) (Scheme 2). This was followed up some years later in the mid 1980s by the preparation of CCS polymers comprised of poly(methyl methacrylate) (PMMA) arms and poly(ethylene glycol dimethacrylate) (PEGDMA) cores [4] by group transfer polymerisation (GTP) (Scheme 2) [5]. It was not until the 1990s that the majority of other

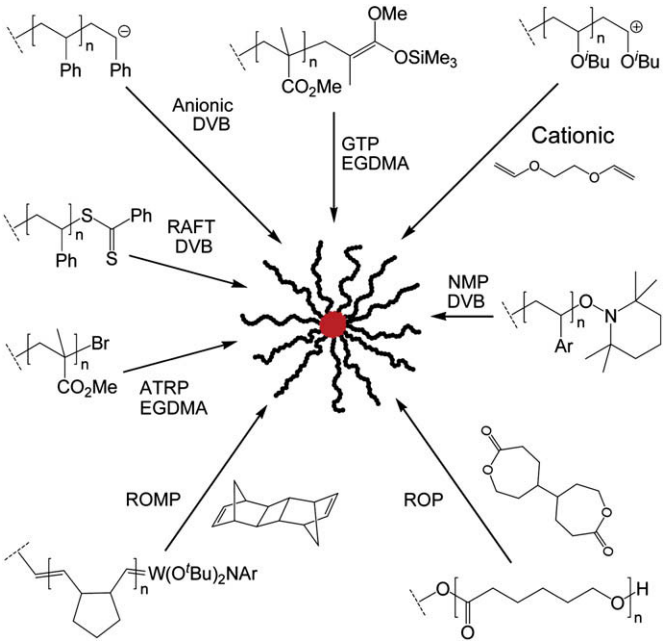

Scheme 2. Synthesis of CCS polymers via the arm-first approach and controlled polymerisation techniques.

controlled polymerisation techniques were exploited for the synthesis of CCS polymers. In 1991, Bazan and Schrock demonstrated that ring-opening metathesis polymerisation (ROMP) of norbornene followed by cross-linking with a norbornadiene dimer formed CCS polymers with quantitative conversion of the living arms (Scheme 2) [6]. In that same year, Kanaoka et al. employed cationic polymerisation to prepare CCS polymers in high yield via the cross-linking of living poly(*iso*butyl vinyl ether) with divinyl ether cross-linkers (Scheme 2) [7]. The introduction of CRP techniques [8–10] that have enabled the production of high molecular weight and low polydispersity polymers from a large range of monomer families and under less stringent reaction conditions dawned in a new era for polymer synthesis. Shortly after their advent, the potential of the CRP techniques of nitroxide mediated polymerisation (NMP) and atom transfer radical polymerisation (ATRP) for the preparation of CCS polymers (Scheme 2) was realised, with patents being filed for both processes by Solomon and co-workers in 1997 [11] and 1999 [12], respectively. Similarly, the application of reversible addition–fragmentation chain transfer (RAFT) polymerisation for the synthesis of CCS polymers was patented in 1999 [12] and 2000 [13], and demonstrated in 2003 (Scheme 2) [14], albeit the polymers formed possessed very broad polydispersities, highlighting issues associated with the chain transfer mechanism of the RAFT approach [15]. Most recently, Wiltshire and Qiao have employed ring-opening polymerisation of lactones to prepare fully degradable CCS polymers [16] with arms and core derived from ε-caprolactone and the bislactone, 4,4′-bioxepanyl-7,7′-dione, respectively (Scheme 2).

Another, less direct, but equally valid method that leads to the formation of 3D polymeric nanostructures that closely resemble CCS polymers involves the core cross-linking and covalent stabilisation of self-assembled core–shell micelles [17,18], which can be regarded as a 'through-approach'. Although CRP techniques have been used for cross-linking of micelle cores, predominantly other types of cross-linking mechanisms (e.g. free radical reactions [19], γ-irradiation [20], cold-vulcanization [21], photoinitiation [22], photodimerisation [23] and multifunctional coupling reagents [24]) have been utilised to prepare CCS-like polymers from preformed micelles and block copolymers in bulk morphologies. For example, Müller and co-workers prepared Janus (non-centrosymmetric or surface-compartmentalised) nanoparticles [25] via the disulfur dichloride mediated cross-linking of ABC tri-block copolymers organised in non-centrosymmetric lamellae [21]. Although Janus nanoparticles are structurally similar to CCS polymers (i.e. they have a cross-linked core from which linear arms radiate outwards), their preparation from MIs (or MMs) via the arm-first CRP techniques introduced previously is unconceivable as the arm-first mechanism does not allow for the pre-organisation that is required and can only be achieved through self-assembly processes. The photodimerisation core cross-linking of core isolated cinnamoyl moieties in block copolymer micelles provided the unique opportunity to determine the degree of cross-linking in the resulting CCS polymers via UV–visible spectroscopy [26]. In comparison, attempts to determine the degree of cross-linking in CCS polymers prepared via the arms-first approach and CRP techniques have been unsuccessful. Although there are many examples of core cross-linking of self-assembled nanostructures via both CRP and non-CRP techniques, the cases discussed above highlight some of the potential differences between the arm-first micelle cross-linking and arm-first MI approaches even though both are capable of yielding macromolecules with very similar architectures.

Regardless of the synthetic approach or polymerisation techniques employed, CCS polymers, and for that matter all star polymers, might be expected to display very similar properties if the properties are governed by the arm constituents and their composition rather than the way in which the stars are complied. Thus, star polymers of identical arm composition and similar arm numbers, but prepared, for example, by arm-first CRP or core-first anionic polymerisation or even micelle core cross-linking maybe chemically and physically (from a peripheral viewpoint) indistinguishable. A prominent example which highlights the similarities of star polymers prepared via different synthetic approaches is the properties of poly(acrylic acid) (PAA) stars with oligosaccharide cores prepared via the core-first approach [27] and cross-linked poly(divinyl benzene) (PDVB) cores prepared via the arm-first approach [28]; both have comparable apparent pK_a values and behave similarly in response to pH changes. In contrast, if the properties of star polymers are influenced by their core structure, composition and size then it is reasonable to deduce that star polymers with discrete cores prepared via the core-first approach will behave differently to star polymers with large cross-linked cores prepared via the arm-first approach.

Given that the preparation and application of CCS polymers have been studied for nearly 40 years it is evident that this is a substantial area of polymer research. As a result, it is outside the scope of this article to provide a comprehensive coverage of this extensive field and the reader is directed to several excellent reviews [2,29–32] and books [33–37] that have been published in recent times. Rather, this review highlights the scientific literature from the late 1990s to the present concerning the development and applications of CCS polymers prepared via CRP techniques and the arm-first approach. Although there have been recent reports on the synthesis of CCS-like polymers via ATRP and the core-first approach [38], the polydispersities of the resulting polymers were significantly broader than those obtained for similar CCS polymers prepared via the arm-first approach. The review will discuss strategies for controlling the macromolecular architecture and functionalisation of CCS polymers, their characterisation, physical properties and applications. Where possible information is provided pertaining to the molecular weight characteristics (e.g. weight-average molecular weight (M_w), polydispersity index (PDI), number of arms (f)) and molecular dimensions (e.g. radius of gyration (R_g), hydrodynamic radius (R_h)) of the CCS polymers, however, it should be noted that the methods of their determination vary considerably and as such, will be denoted by the

appropriate abbreviation; M_w values determined using multi-angle laser light scattering (MALLS) will be denoted as $M_{w(MALLS)}$, whereas M_w values determined using a conventional calibration with linear standards, or a universal calibration with a triple detector system will be donated as $M_{w(CC)}$ and $M_{w(UC)}$, respectively.

2. Synthesis of CCS polymers via CRP

As a result of the stringent reaction conditions and limited range of monomers [39,40], the use of living anionic and cationic polymerisation to prepare CCS polymers has been superseded by recent developments in CRP techniques, which allow complex macromolecules with high degrees of functionality and compositional variation to be prepared under relatively facile conditions [2]. The CRP techniques that have been successfully implemented include NMP, ATRP and RAFT polymerisation, although it is prominent that they each have different advantages and disadvantages, which are inherent of the particular technique [41–43].

The proposed mechanism of CCS polymer formation from living MIs and a divinyl cross-linker consists of the initial addition of the cross-linker to the MIs to form short block copolymers (Scheme 3). The block copolymers can then react with more cross-linker, MIs or with the pendent vinyl groups present on other block copolymers. As more and more of the block copolymers link together they begin to form a star polymer with a lightly cross-linked core. If the cores of these star polymers are sterically accessible to each other then star–star coupling can occur resulting in the formation of higher molecular weight macromolecules. Simultaneously, block copolymers and MIs could also add to these lightly cross-linked star polymers. Once the majority of the block copolymers have been immobilised into the star structure it is likely that intramolecular cross-linking within the stars dominates to afford CCS polymers with denser cross-linked cores. Evidence for the formation of these block copolymers containing pendent vinyl groups has been observed from ^{1}H NMR spectroscopic analysis [44–47] of samples taken at short reaction times, which, after isolation of the polymeric material, revealed characteristic vinylic proton resonances. In comparison, ^{1}H NMR spectra of CCS polymers are dominated by resonances corresponding to the arms and lack resonances corresponding to the core and pendent vinyl groups. Such results are consistent with the formation of star-shaped polymers with mobile arms and rigid cores. Although it is likely that there are still pendent vinyl groups present within the cores of the CCS polymers, it is expected that they will not be detected by ^{1}H NMR spectroscopic analysis given the reduced segmental mobility of the core.

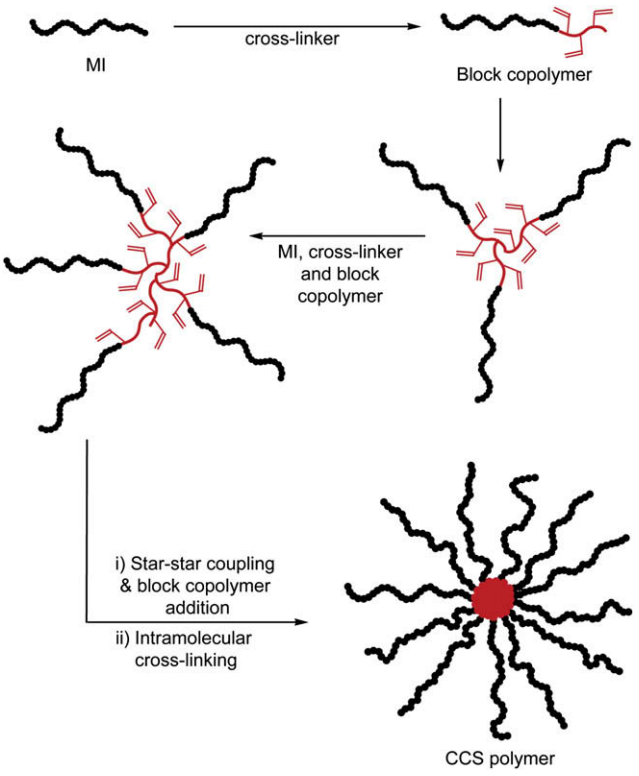

Scheme 3. Proposed mechanism for the formation of CCS polymers from living MIs and cross-linker.

One of the major drawbacks of CRP for the preparation of CCS polymers is that generally not all of the MIs react to form star polymer. Although the extent of MI (or MM) to CCS polymer conversion (star yield) can be tailored by careful manipulation of the reaction conditions or special protocols [48], it is very rare that quantitative conversion has been achieved [49]. Therefore, fractional precipitation is commonly employed to purify the crude polymerisation mixtures, affording the desired CCS polymers with relative ease given the large difference in molecular weight that exists between the components of the mixture. In general, the preparation of CCS polymers via CRP is accompanied by some low molecular weight materials that maybe either unconverted MIs or block copolymers. Although it is evident that this low molecular weight material may originate from MIs that have lost their living functionality (during their synthesis), in cases where the MIs 'livingness' has been deemed 100% from chain extension experiments several theories can be proposed as to its incomplete conversion to CCS polymer: (i) The formation of dead chains from MIs due to radical termination events prior to the addition of cross-linker; (ii) Initially, all of the MIs are converted to block copolymers via chain extension to some extent by the addition of cross-linker, but due to the steric congestion around the cores of the preformed CCS polymers, not all are incorporated. However, this raises the question, if there are remaining block copolymers present why do they not subsequently react to form new star polymers? One answer could be that the remaining block copolymers have lost their living ends, and as there are no living ends capable of producing radicals outside of the inaccessible preformed CCS polymer cores they cannot link together to form new stars; (iii) If chain extension of the MIs with the cross-linker is unequal (i.e. some block copolymers have a large number of pendent vinyl groups, whilst others have very few) then it would be expected that the block copolymers with a larger number of pendent vinyl groups would predominantly react to form CCS polymers, leaving block copolymers with very few pendent vinyl groups present. As a result of the decreased concentration of these block copolymers and the small number of vinyl groups, the probability of cross-linking reactions decreases whilst the probability of radical termination events increases.

Although several studies have shed some light on the nature of this low molecular weight material, none have conclusively proven one mechanism over another. In theory, it is conceivable that all of the mechanisms proposed play a role to some extent. For example, Baek et al. conducted ^{1}H NMR spectroscopic analysis [45] of the low molecular weight material after its isolation from a CCS polymer reaction mixture, which revealed the presence of unreacted vinyl groups and indicated that its exclusion from the CCS polymer was not due to the loss of the MI living ends before the addition of some cross-linker. However, the apparent lack of increase in molecular weight of this low molecular weight material from the pure MI implied that the addition of cross-linker was low and may not have added to all the MIs [45]. Similarly, Spiniello et al. isolated the low molecular weight material present after the formation of CCS polymers from a MI, cross-linker and mono-vinyl fluorescent monomer [50]. Gel permeation chromatography (GPC) analysis of

this material revealed a significant increase in molecular weight relative to the pure MI and online UV–visible measurements revealed absorptions corresponding to the fluorescent monomer (Fig. 1). Given the observed increase in molecular weight, it was concluded that the majority of the MIs had been chain extended with some cross-linker as the increase in molecular weight could not result from the sole addition of the fluorescent monomer.

The nature of the low molecular weight material may not seem that important given that the desired component of the reaction is the CCS polymer. However, the way in which it is perceived does have a slight effect on the calculation of the *f* of the star and therefore, the core molecular weight. For example, the value calculated for the *f* may vary depending on the assumption that (i) all of the cross-linker consumed in the reaction adds evenly to all the MI (i.e. there is some cross-linker present in the low molecular weight material) or (ii) that all of the cross-linker is incorporated into the CCS polymer and that none is present in the low molecular weight material. Based on these assumptions the *f* can be calculated according to Eq. (1) or (2), respectively:

$$f \approx \frac{M_{w(CCS)}}{\left(([CL]/[MI]) \times \text{Mol. wt.}_{(CL)} \times X_{(CL)}\right) + M_{w(MI)}} \quad (1)$$

$$f \approx \frac{WF_{(arm)} \times M_{w(CCS)}}{M_{w(MI)}} \quad (2)$$

where $M_{w(CCS)}$ and $M_{w(MI)}$ are the weight-average molecular weights of the CCS polymer and MI, respectively, Mol. $wt._{(CL)}$ is the molecular weight of the cross-linker, $X_{(CL)}$ is the fractional conversion of cross-linker, [CL]/[MI] is the molar ratio of cross-linker to MI and $WF_{(arms)}$ is the weight fraction of arms in the CCS polymer as determined by Eq. (3):

$$WF_{(arms)} = \frac{\frac{[MI]}{[CL]} \times M_{w(MI)} \times X_{(MI)}}{\text{Mol. wt}_{(CL)} \times X_{(CL)} + \frac{[MI]}{[CL]} \times M_{w(MI)} \times X_{(MI)}} \quad (3)$$

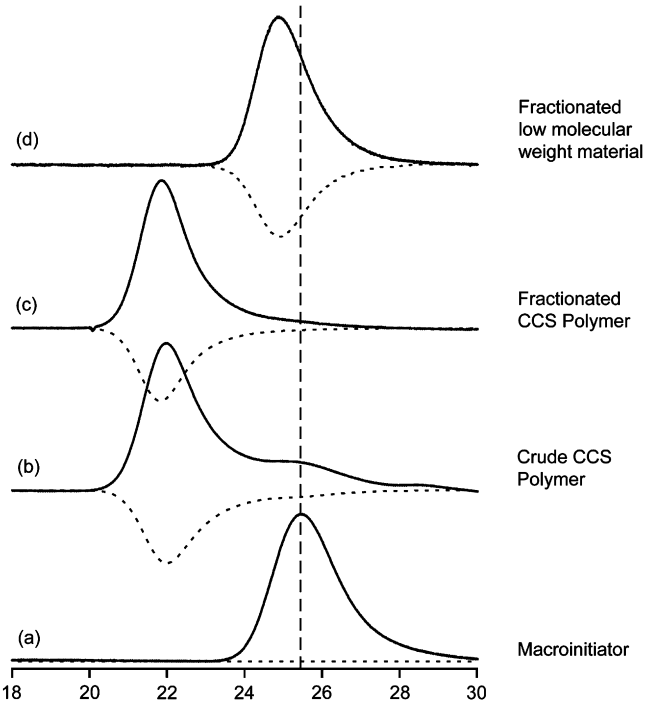

Fig. 1. GPC RI (—) and UV (---) ($\lambda = 343$ nm) traces for (a) PMMA MI, (b) crude fluorescent CCS polymer, (c) fractionated fluorescent CCS polymer and (d) fractionated low molecular weight material [50].

where $X_{(MI)}$ is the fractional conversion of MI to CCS polymer (usually determined by GPC RI analysis). If the conversion of MI to CCS polymer is high then the *f* calculated from Eqs. (1) and (2) will be in good agreement. However, as the conversion of MI to CCS polymer decreases, the *f* calculated from Eq. (1) remains constant, whereas the *f* calculated from Eq. (2) decreases. This difference results from the number of cross-linker molecules added to each MI incorporated into the CCS polymer remaining constant regardless of the conversion of MI in Eq. (1), whereas, for Eq. (2) the number of cross-linker molecules added to each MI incorporated into the CCS polymer increases as the MI conversion decreases. In turn, this also affects the calculation of the core molecular weight as this is related to the *f* by Eq. (4).

$$M_{w(core)} \approx M_{w(CCS)} - \left(M_{W(MI)} \times f\right) \quad (4)$$

The calculation of the *f* can also be complicated by the introduction of additional groups, such as spacers or functional groups, into the core. For example, if a cross-linker and mono-vinyl monomer are employed during the cross-linking, core formation step, then the incorporation of the both components into the core should be considered when determining the *f*. This can be achieved via two approaches depending on how the incorporation of the additional group has been determined. If the statistical distribution of the additional groups per macromolecule has been determined by analytical methods post-synthesis and isolation of the CCS polymer (such as a core isolated chromophore) then Eq. (5) can be employed:

$$f \approx \frac{M_{w(CCS)} - \left(\text{Mol. wt.}_{(AG)} \times \left(\text{mol.}_{(AG)}/\text{mol.}_{(CCS)}\right)\right)}{\left(([CL]/[MI]) \times \text{Mol. wt.}_{(CL)} \times X_{(CL)}\right) + M_{w(MI)}} \quad (5)$$

where Mol. $wt._{(AG)}$ is the molecular weight of the additional group and the term $mol._{(AG)}/mol._{(CCS)}$ refers to the loading of the additional group. Alternatively, the incorporation and conversion of the additional group during core formation may have been determined in a similar manner to which the conversion of the cross-linker was calculated. In which case, Eq. (1) or (3) can be modified to account for this additional component. For example, Eq. (6) is a derivative of Eq. (1) which accounts for the incorporation of the additional group, but presumes a statistical distribution of this group to both the CCS polymer and the unconverted low molecular weight material;

$$f \approx \frac{M_{w(CCS)}}{m_{(CL)} + m_{(AG)} + M_{w(MI)}}$$
$$m_{(CL)} = \left(([CL]/[MI]) \times \text{Mol. wt.}_{(CL)} \times X_{(CL)}\right)$$
$$m_{(AG)} = \left(([AG]/[MI]) \times \text{Mol. wt.}_{(AG)} \times X_{(AG)}\right) \quad (6)$$

where $m_{(CL)}$ and $m_{(AG)}$ are the mass contribution of the cross-linker and additional groups to each of the macroinitiators, respectively. It should be noted that although Eqs. (1)–(6) are based on M_w values, it is also valid to use number-average molecular weight (M_n) and peak molecular weight (M_p) values. In theory, a more accurate determination of the *f* can be obtained by calculations based on the M_n, however, absolute M_w values determined from light scattering measurements are more accurate than the number-average counterparts obtained by membrane osmometry or other methods. Furthermore, the *f* actually represents the average number of arms, as CCS polymers are not uniform in arm number, but involve a statistical distribution of arm numbers.

2.1. NMP and metal catalysed ATRP

The construction of CCS polymers via NMP and metal catalysed ATRP generally involves the preparation of a living MI followed by cross-linking with a divinyl (or higher) cross-linker in either a one-pot or two-pot strategy. Whereas the one-pot strategy involves the addition of cross-linker to the MI formation reaction at a certain monomer conversion, the two-pot strategy involves synthesis and isolation of the MI followed by a second reaction with cross-linker. To maintain a high proportion of living polymer chains in the initial stage of the two-pot strategy, the synthesis of the MI is stopped prior to complete consumption of the monomer (as side reactions become apparent at low monomer concentrations) [43]. Evidently, the one- and two-pot strategies lead to CCS polymers with slightly different cross-linking densities within the core as a result of the incorporation of a spacer group (the monomer remaining from the MI synthesis) in the one-pot strategy. Similarly, the preparation of CCS polymer via RAFT polymerisation utilises a MI terminated with a chain transfer agent. An alternative to MIs, recently reported by Gao et al., utilises MMs in the presence of a small molecule initiator and cross-linker to prepare CCS polymers via ATRP [48].

The synthesis of CCS polymers by NMP was first reported by Solomon and co-workers [51] who employed the alkoxyamine initiator **1** derived from 2,2′-azobis(2-methylpropionitrile) (AIBN), 2,2,6,6-tetramethylpiperidine-1-oxyl (TEMPO) and 4-*t*-butylstyrene (*t*-BSt) to firstly prepare linear poly(4-*t*-butylstyrene) (P^{t}BSt) of various DP before cross-linking with either DVB [40] or a mixture of DVB and *t*-BSt (Scheme 4) [51,52]. GPC RI analysis of the CCS polymers formed via both approaches revealed broad multi-modal traces. When DVB was employed in the cross-linking step the resulting mixture was found to contain residual linear precursors, whereas the copolymerisation of both DVB and TBS resulted in considerable inter-particle or star–star coupling and the formation of CCS polymers with very broad polydispersities. The NMP approach has since been refined by the introduction of improved alkoxyamine functionalised initiators [53,54], which have permitted the use of a wide range of monomer families and enabled the production of narrow polydispersity CCS polymers, in high yield, using a variety of alkoxyamine terminated MIs.

The successful application of copper and ruthenium mediated ATRP (ATRP$_{(Cu)}$ and ATRP$_{(Ru)}$, respectively) for the preparation of CCS polymers was first reported by Matyjaszewski et al. [55] and Sawamoto et al. [45] via the one-pot and two-pot strategies, respectively. Unlike the initial problems encountered by Solomon and co-workers with NMP [51,52], ATRP was found to be much more versatile, readily facilitating the preparation of well-defined CCS polymers in high yields.

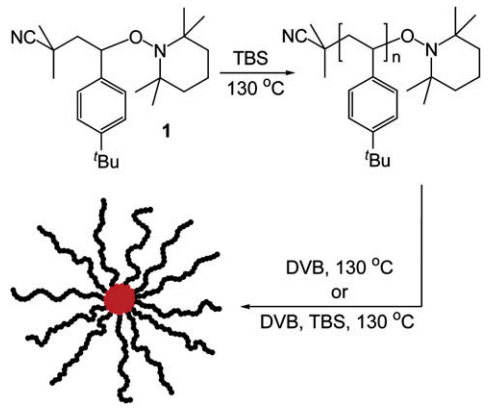

Scheme 4. Synthesis of P^{t}BSt$_{arm}$PDVB$_{core}$ CCS polymers via NMP [51,52].

2.2. RAFT polymerisation

Initial attempts to apply RAFT polymerisation for the preparation of CCS polymers from dithiobenzoate terminated living PSt and DVB [14] lead to the formation of macromolecules with broad polydispersities as a result of side reactions involving the intermediate radicals [56] and potentially, core and chain shielding effects [57]. For example, the reaction of a PSt dithiobenzoate chain transfer MI with DVB in a 1:35 molar ratio leads to the formation of a CCS polymer ($M_{w(CC)} = 60.3$ kDa) with a PDI of 2.93 [58]. GPC RI analysis of the reaction after 9 h revealed two relatively well-defined peaks corresponding to the MI and CCS polymer ($M_{w(CC)} = 16.2$ kDa, PDI = 1.62) in a 1:1 ratio. Although the yield of CCS polymer continued to increase with reaction time, reaching a maximum of *ca.* 90% after 46 h, the GPC RI trace became increasingly broad and multi-modal in appearance. The slow consumption of MIs in the initial stages of the reaction (relative to ATRP and NMP reactions) was attributed to the difference in the polymerisation mechanism as a result of the addition–fragmentation equilibrium of the RAFT process [56]. Given that linear polymer chain radicals can attack dithiobenzoate groups in lightly cross-linked star polymers to release dithiobenzoate terminated linear polymer chains and vice versa, it is understandable that the linear polymers are consumed slowly. Once most of the DVB has been consumed reactions between CCS polymers occur as a result of the high proportion of dithiobenzoate groups located within the core, which leads to the polymerisation of DVB and/or pendent vinyl groups. Hence, the appearance of a high molecular weight peak in the GPC traces and the observed increase in PDI. When the DVB/MI molar ratio was varied from 3 to 35, the molecular weight, PDI and CCS polymer yields all increased. Similarly, Zhang and Chen prepared a PSt$_{arm}$DVB$_{core}$ CCS polymer ($M_{w(CC)} = 87.0$ kDa, PDI = 3.47) using telechelic homopolymers derived from a bisallyl trithiocarbonate chain transfer reagent [59]. Once again, broad polydispersities were observed as a result of the chain transfer mechanism [57]. Recent developments for the RAFT process have taken advantage of solvent control and micelle formation prior to, or during, cross-linking to afford well-defined CCS polymers with low polydispersities [60].

3. Structural control and diversity

3.1. Structural control

Given the large number of variables associated with the preparation of CCS polymers it is evident that optimisation and appreciation of structural control in these systems offer considerable challenges to the synthetic polymer scientist. In addition to the type of CRP technique employed, the structure (molecular weight, *f*, R_g and core size) and yield (conversion of MI to CCS polymer) of CCS polymers are dictated by a wide variety of experimental factors, namely the type of MI (or MM) and cross-linker used, the type of catalyst and catalyst–ligand complex (ATRP), the DP of the MI, the molar ratio of cross-linker to MI, the concentration of the MI, the incorporation of a spacer group during core formation and the nature of the solvent.

Three of the most important considerations when preparing CCS polymers are the cross-linker/MI molar ratio, the concentration of MI and the DP of the MI. However, in turn, these variables are affected somewhat by the structure and reactivity of the cross-linker, and the structural composition of the MI. Regardless of these complexities some general trends can be noted; for example, an increase in the cross-linker/MI molar ratio or MI concentration, up to a certain point, leads to an increase in CCS polymer molecular weight and yield. Further increases result in the formation of star–star coupled products with broad polydispersities and even

insoluble gels. Increasing the DP of the MI usually results in a decrease in the molecular weight and yield of the CCS polymer. These trends are highlighted by the results (Fig. 2) of a simple study involving the reaction of PMMA MIs with ethylene glycol dimethacrylate (EGDMA) via $ATRP_{(Cu)}$ [61]. As the DP of the MI was increased the $M_{w(UC)}$ values of the resulting CCS polymers first decreased then gradually increased, whilst the *f* decreased and plateaued (Fig. 2a), and the yield of star continuously decreased (Fig. 2d). When the cross-linker/MI ratio or MI concentration was increased, the $M_{w(UC)}$ values of the CCS polymers increased exponentially (Fig. 2b and 2c, respectively), which corresponds to an increase in the *f*. Similarly, the yield of CCS polymer was also found to increase with increasing cross-linker/MI ratio, whereas the yield initially increased up to a certain point and then decreased as the concentration of MI was increased (Fig. 2d).

3.1.1. CCS polymers via ATRP

For $ATRP_{(Cu)}$, Matyjaszewski and co-workers established that cross-linker (DVB)/MI molar ratios of between 5 and 15 were optimal for the formation of CCS polymers from PSt [55] and poly(*t*-butyl acrylate) (P^tBA) MIs [62]. Whereas the yield and molecular weight of the CCS polymers were found to increase with an increase in DVB, higher ratios of DVB/MI (>15) led to significant broadening of the molecular weight distribution and, for the DVB/PSt system, insoluble gel formation. Several other factors pertinent to the preparation of CCS polymer via $ATRP_{(Cu)}$ were also examined, including the effect of the divinyl cross-linker, catalyst–ligand complex, choice of exchange halogen, reaction medium and reaction time [55,62]. Using a PSt MI it was observed that DVB leads to the formation of soluble CCS polymers, whereas 1,4-butandiol diacrylate (BDDA) and EGDMA resulted in the formation of insoluble gels [55]. Similar results were obtained when a P^tBA MI was employed, with the exception that BDDA led to the formation of soluble CCS polymers with high molecular weight and broad polydispersities [62]. In both cases DVB resulted in the formation of stars with relatively narrow polydispersities. The effect of the type of copper–ligand complex on the molecular weight and yield of CCS polymers prepared from a PSt MI and DVB was found to be minimal, although the rate of reaction was found to be higher when *N*,*N*,*N*′,*N*″,*N*″-pentamethyldiethylenetriamine (PMDETA) was used in place of 2,2′-bipyridine (bpy), which was ascribed to the lower redox potential of the formers' copper complex [55]. For the preparation of CCS polymers from P^tBA MIs and DVB the choice of solvent also proved to be significant, given that reactions in non-polar solvents such as benzene resulted in the formation of some insoluble gels, whereas reactions conducted in polar solvents such as 1,2-dichlorobenzene and ethyl acetate afforded soluble polymers of similar molecular weights and yields [62].

In a series of publications [45,46,63] Sawamoto and co-workers examined the one-pot synthesis of CCS polymers via $ATRP_{(Ru)}$,

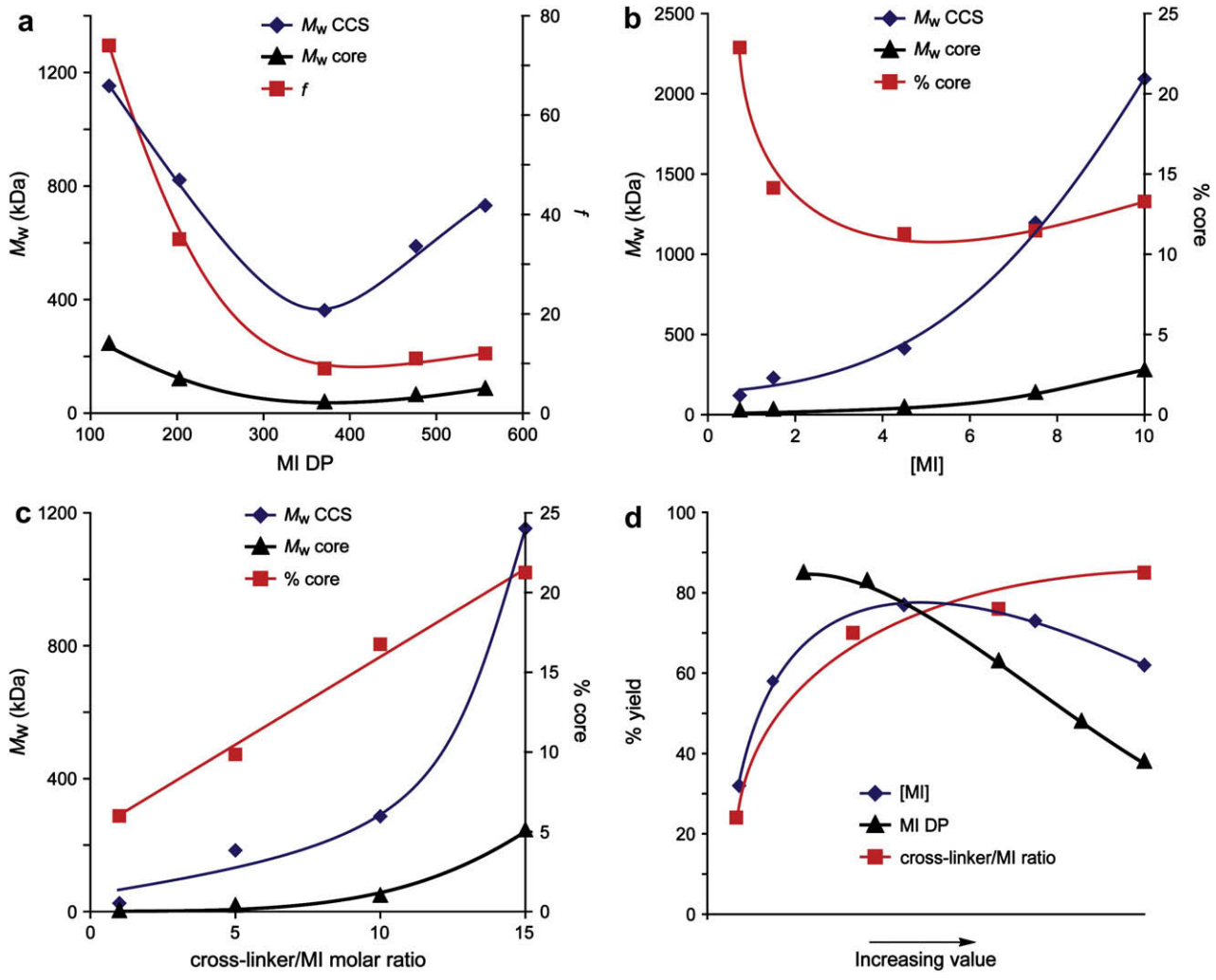

Fig. 2. General trends observed for the preparation of $PMMA_{arm}PEGDMA_{core}$ CCS polymers via $ATRP_{(Cu)}$ [61].

investigating such variables as the type of cross-linker, cross-linker/MI molar ratio, MI DP, MI concentration, reaction temperature, solvent nature and catalyst concentration. Firstly, PMMA MI was prepared and at a MMA conversion of *ca.* 90% various cross-linkers, including both dimethacrylates **2**–**7** [45] and di(meth)-acrylamides **8**–**14** [34] (Fig. 3) were added in a cross-linker/MI molar ratio of 10. Whereas the dimethacrylate cross-linkers **2**–**5** all resulted in the formation of CCS polymers in relatively high yield, negligible reaction was observed for cross-linkers **6** and **7**. The poor conversions obtained with cross-linker **6** were attributed to the flexible trioxyethylene spacer, which favours intramolecular cyclisation reactions. Interestingly, the most effective dimethacrylate cross-linker, **2** (bisphenol A dimethacrylate (BAM)), for the formation of CCS polymers from PMMA MIs, proved to be ineffective when a poly(*n*-butyl acrylate) (P^nBA) MI was employed, highlighting the importance of choosing an appropriate cross-linker–MI combination [45]. All of the diacrylamide cross-linkers afforded CCS polymers in good yields (>76%), with the exception of the dihydroxyl cross-linker **12**. For the diacrylamides **8**–**11** the yields and molecular weights of the CCS polymers were found to decrease as the spacer length was increased, whereas the bulky diacrylamide **14** afforded a star with very high molecular weight ($M_{w(MALLS)}$ = 1.5 MDa, $f \approx 82$), in high yield, after just 2 h of reaction. The effect of PMMA MI DP and cross-linker/MI molar ratio was studied using the cross-linkers BAM and **8** [46,63]. When the cross-linker/MI ratio was increased whilst the DP of the MI remained fixed, the yield and molecular weight of the CCS polymers increased, which corresponded to an exponential increase in the *f*. Similarly, an increase of PMMA DP at a fixed cross-linker/PMMA molar ratio also resulted in an increase in the yield and molecular weight of the CCS polymers, however, the *f* remained relatively constant. For the cross-linker BAM the PMMA MI concentration was also increased incrementally whilst the PMMA DP and cross-linker/PMMA molar ratio remained fixed, which was found to result in an increase in the yield and molecular weight of the CCS polymers [63]. In addition, it was determined that the rate of the cross-linking reaction could be increased by raising the reaction temperature, using more polar solvents or higher catalyst concentrations [63]. Although higher catalyst concentrations resulted in a faster coupling reaction, it is worth noting that over extended reaction times lower yields of CCS polymers were achieved relative to reactions conducted with lower catalyst concentrations.

Furthermore, Sawamoto and co-workers assessed the possibility of using an iron(II) catalyst ($FeCl_2(PPh_3)_2$) for the preparation of CCS polymers from PMMA MI and BAM [45], however, the catalyst exerted poor control over the polymerisation, resulting in the formation of high molecular weight products with very broad polydispersities.

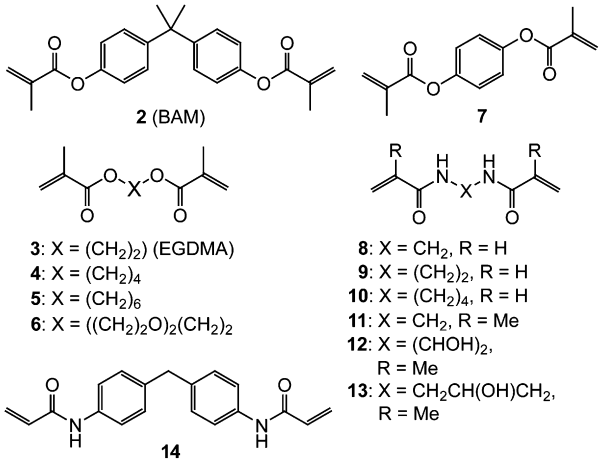

Fig. 3. Cross-linkers employed for the synthesis of CCS polymers via $ATRP_{(Ru)}$ [45,46,63].

Similar structure studies have also been conducted by Gao and Matyjaszewski via $ATRP_{(Cu)}$ and a one-pot strategy, in which various amounts of DVB were added during the preparation of linear P^tBA at certain *t*-BA conversions [64]. Initially, the effect of P^tBA DP was investigated by fixing the amount of unreacted *t*-BA and DVB. As the DP of the MI was varied from 90 to 20 the molecular weight values ($M_{w(MALLS)}$ = 70.6–142.9 kDa, $f \approx 5$–34) of the resulting CCS polymers increased, which was accompanied by an increase in the PDI from 1.23 to 1.84. Thus, indicating that the larger MIs have poor mobility and sterically hinder the incorporation of a large number of arms into individual CCS macromolecules, which is also demonstrated by the decrease in yield with increasing DP. Furthermore, the lower extent of MI incorporation observed at high DP leads to a smaller core and looser structure as evidenced by measurements of the polymers' compactness ($M_{p(MALLS)}/M_{p(CC)}$), for which a more compact structure would result in a higher value. For example, CCS polymers prepared from P^tBA MIs with DPs of 20 and 90 possessed compactness values of 2.11 and 1.20, respectively. Secondly, the influence of DVB addition at particular *t*-BA conversions (60, 80 and 90%) was examined by fixing the total amount of *t*-BA and DVB. When DVB was added at low *t*-BA conversion the resulting CCS polymer had a high $M_{w(MALLS)}$ (126.5 kDa, $f \approx 19$) and broader PDI (1.56) relative to the polymer ($M_{w(MALLS)}$ = 32.1 kDa, $f \approx 5$, PDI = 1.24) formed when DVB was added at high *t*-BA conversion. Although the addition of DVB at low *t*-BA conversion leads to a decrease in the cross-link density of the star core, it also facilitates the incorporation of more arms as a result of their smaller size and increased mobility. Therefore, CCS polymers prepared by the addition of DVB at low *t*-BA conversion possessed higher values of compactness. Finally, the amount of DVB was varied at a fixed total amount of *t*-BA and *t*-BA conversion of 80%. An increase in the DVB/MI molar ratio from 1.5 to 15 resulted in an increase in the yield (72–95%), $M_{w(MALLS)}$ (28.1–676.4 kDa, $f \approx 5$–87) and PDI (1.22–3.86) of the resulting CCS polymers. Correspondingly, the compactness (1.16–5.18) of the polymers increased as the *f* increased. For comparative purposes P^tBA CCS polymers with only PDVB cores were also prepared via a two-pot process, in which pre-isolated P^tBA MIs were reacted with various amounts of DVB without the addition of *t*-BA as a spacer group. Although the CCS polymers prepared via the two-pot process possessed lower $M_{w(MALLS)}$ values (27.3–365.5 kDa, $f \approx 5$–54) they also had much lower PDI values (1.15–1.54). Interestingly, at low ratios of DVB/MI significantly higher yields of CCS polymer were obtained by the one-pot approach, whereas the difference was less pronounced at higher ratios, indicating that the incorporation of a spacer group during the cross-linking step has a pronounced effect on the formation of CCS polymer.

Several factors effecting the formation of amphiphilic CCS polymers consisting of poly(ethylene oxide) (PEG) arms and PDVB cores have been investigated via $ATRP_{(Cu)}$. Using a 2-bromoisobutyryl functionalised PEG MI and DVB (tech. grade 45%) Du and Chen observed that the $M_{n(CC)}$ (26.1–42.6 kDa) and yield (10–83%) of CCS polymers increased as the DVB/MI molar ratio was increased from 4.7 to 20 [65]. Chen et al. employed distilled DVB in their study and revealed similar trends as the DVB/PEG molar ratio was increased from 5 to 15, with the exception that the resulting CCS polymers ($M_{n(CC)}$ = 20.1–61.2 kDa, PDI = 10.8–1.15) could be obtained in high yields (up to 99%) [66]. The choice of solvent also played an important role, with benzene, anisole and chlorobenzene resulting in the formation of CCS polymers with broad PDI (>1.48) [66]. In comparison, *o*-xylene afforded stars with narrow PDI (1.12) and in near quantitative yield (>99%).

An interesting alternative to the commonly used arm-first MI approach, which allows for the production of CCS polymers in high yield and low polydispersity, is the MM approach. Whereas the MI

approach has the limitation that the number of initiating sites cannot initially be less than the polymer used for the arm, the MM approach allows the amount of initiator to be adjusted independently of the arm number. As a result the number of initiating sites in the core can be decreased, which limits the extent of star–star coupling reactions. For example, the synthesis of $P^nBA_{arm}PDVB_{core}$ CCS polymers using P^nBA MMs in the presence of the initiator, ethyl 2-bromopropionate and DVB was investigated at a molar ratio of 5:1:15 via $ATRP_{(Cu)}$ (Scheme 5) [48]. Although all of the DVB was consumed after the first 24 h, the yield of CCS polymer continued to increase up to 130 h to afford a star with the $M_{w(CC)}$, PDI and yield of 63.0 kDa, 1.15 and 77%, respectively. In contrast, the corresponding CCS polymer prepared from a P^nBA MI and DVB in a ratio of 1:3 possessed a much broader PDI of 1.55. This difference in PDI was accounted for by consideration of the extent of star–star coupling reactions caused by the amount of initiator present. For the MM system the congestion around the core of the preformed star polymer after 7.5 h prevented star–star coupling and only allowed star–MM reactions, which was attributed to the lower amount of initiator employed. In contrast, star–star coupling reactions occurred throughout the polymerisation for the MI system as the number of initiating sites was higher. To increase the conversion of MM to CCS polymer additional batches of DVB and initiator were added periodically. After 4 additions the majority of the MM had reacted to afford CCS polymer ($M_{w(MALLS)} = 466.0$ kDa) in a yield of 98%, whilst the PDI (1.19) only increased slightly. Although it is evident that any unreacted MM can react not only with the core of preformed stars, but also the newly added DVB and initiator to form primary MI, GPC analysis revealed that the newly formed MI reacted preferentially with initiating sites or vinyl groups in the preformed star cores rather than with each other to form new stars. To demonstrate the flexibility of the MM approach $PEG_{arm}PEGDMA_{core}$ CCS polymers were also prepared using PEG MMs, ethyl 2-bromo*iso*butyrate as the initiator and EGDMA in a molar ratio of 10:1:10. After 29 h of reaction the yield of star polymer had reached 97% and possessed a PDI of 1.18.

3.1.2. CCS polymers via NMP

Following on from the preliminary studies of Solomon and co-workers [51,52] several research groups have conducted detailed examinations into the preparation of CCS polymers via NMP [67–69]. The effects of cross-linker/MI molar ratio, MI DP and reaction time on the structure and yield of CCS polymers prepared via NMP were investigated by Hadjichristidis and co-workers [68]. It was noted that in order to obtain $PSt_{arm}PDVB_{core}$ CCS polymers in good yields (75%), long reaction times (8–10 days) were required. Variation of the TEMPO terminated PSt MIs M_w from 9.7 to 70.0 kDa, at a fixed DVB/MI molar ratio of 13, leads to a decrease in the M_w, f and yield of star. When the DVB/MI ratio was increased from 6.5 to 13 using a PSt MI with a M_w of either 15.0 or 34.0 kDa the yields and M_w values of the CCS polymers were found to increase. Remarkably, Pasquale et al. observed that a very high DVB/TEMPO terminated PSt MI ($M_{n(UC)} = 19.3$ kDa, PDI = 1.10) molar ratio of 68 and reaction time of 24 h were required to successfully form a CCS polymer ($M_{n(UC)} = 319.0$ kDa, PDI = 3.03, 77%), albeit the polydispersity was very broad [67]. Longer reaction times were found to result in an increase in the polydispersity without any further increase in the yield of CCS polymer.

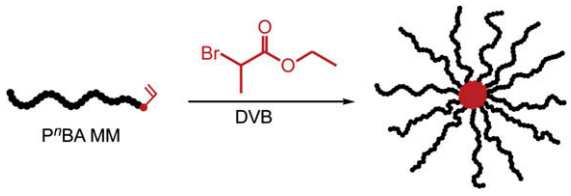

Scheme 5. Synthesis of $P^nBA_{arm}PDVB_{core}$ CCS polymers using P^nBA MMs, ethyl 2-bromopropionate and DVB via $ATRP_{(Cu)}$ [48].

One of the most ingenious approaches towards determining the optimum conditions and structural diversity of CCS polymers was presented by Hawker and co-workers through the application of a high-throughput combinatorial technique [69]. Using a computer-based planning and robotic dispensing system, a series of 96-element libraries were produced to examine the reaction of α-hydrido alkoxyamine terminated PSt MIs with the cross-linker 1,1′-(methylenedi-4,1-phenylene)bismaleimide (BMI) in the presence of styrene as a spacer group. For the first library the BMI and styrene/MI molar ratios were varied simultaneously for a MI of fixed DP and it was established that a BMI/MI molar ratio of 2.75–3.5 at a styrene/MI molar ratio of 2–15 was optimum for the synthesis of well-defined high molecular weight CCS polymers. Taking the lead reaction conditions obtained from the first library, more variables, including the MI DP and concentration, were investigated in subsequent libraries. As a result of these evaluations it was established that as the DP of the MI increased, the amount of BMI required to afford well-defined high molecular weight CCS polymers also increased, with the optimum M_w of the MI being between 3.5 and 9.1 kDa. Furthermore, similar libraries were constructed using DVB as the cross-linker and revealed general trends analogous to the BMI system, with the exception that larger amounts of DVB were required for optimised CCS polymer formation [69].

Amamoto et al. employed a novel approach for the preparation of CCS polymers using radical crossover reactions of alkoxyamine functionalised diblock copolymers [70]. Given the thermally reversible exchange reaction of the complementary alkoxyamine units the diblock copolymer, PMMA-*b*-P(MMA-*co*-**15**-*co*-**16**) **P1** (Scheme 6), could be interconverted between the diblock copolymer and CCS polymer. The diblock copolymers were prepared via $ATRP_{(Cu)}$ using PMMA MIs to initiate the random polymerisation of MMA and methacrylic esters **15** and **16** with complementary alkoxyamine moieties. In total, four diblock copolymers were synthesised with different structures, such as the DP of each block and the composition of the random block. Subsequently, the diblock copolymers were heated at 100 °C at a concentration of 5 wt% to facilitate the radical crossover reaction and formation of the CCS polymers. Time dependent GPC analysis and HPLC quantification of the alkoxyamine **17** generated during the radical crossover reaction revealed that the reaction reached equilibrium after 24 h with the majority of the linear copolymers being converted to CCS polymer. The molecular weight and yield of the CCS polymers were found to be strongly dependent on the concentration, as well as the composition and molecular weight of the diblock copolymer. For example, an increase in the concentration of the diblock from 1 to 10 wt% resulted in an increase in the molecular weight of the resulting stars. The conversion of CCS polymer back to the parent diblock copolymers was investigated through reaction with an excess of the alkoxyamine **17**. The success of the reverse cross-linking reaction was related to the cross-link density of the core. CCS polymers with high cross-linking density underwent a relatively small amount of reverse cross-linking, whereas those with lower cross-linking density almost completely reverted back to the parent diblock copolymer after 48 h.

3.1.3. CCS polymers via RAFT polymerisation

Usually the RAFT polymerisation of chain transfer MIs with cross-linkers results in CCS polymers with broad polydispersities, however, Pan and co-workers have demonstrated that low polydispersity CCS polymers can be prepared via solvent control and the *in situ* formation of block copolymers which undergo aggregation and micelle formation [71–73]. For example, a dithiobenzoate

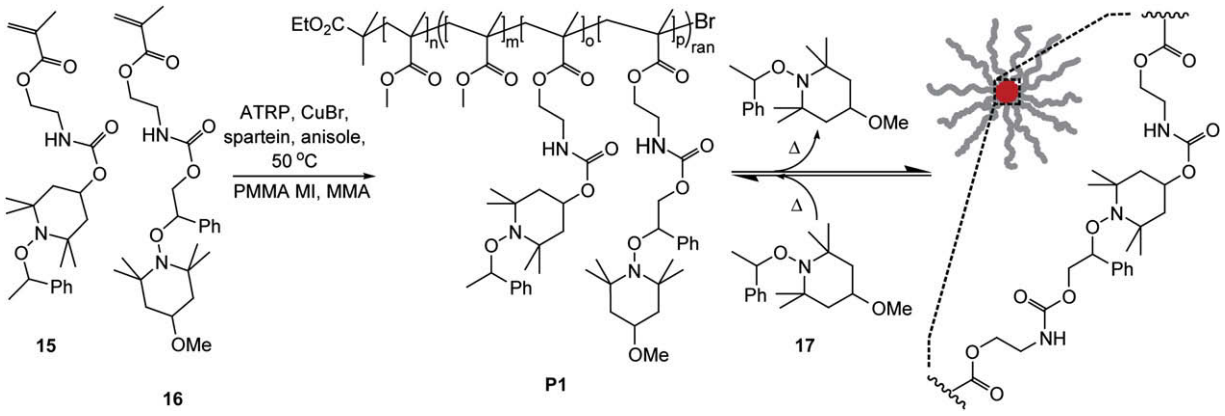

Scheme 6. Synthesis of CCS polymer with thermally reversible dynamic cross-links [70].

terminated PEG chain transfer MI was reacted with styrene and DVB in a 5:1 v/v ethanol:THF mixture using AIBN as the initiator to afford a CCS polymer ($M_{n(CC)} = 81.9$ kDa) with a narrow PDI of 1.09 [72]. The importance of the solvent composition was highlighted by similar reactions conducted in THF, a good solvent for both PEG and P(St-*co*-DVB), and 1:1 water:THF, which after *ca.* 24 h resulted in gel formation and polymers with broad polydispersities, respectively. Similarly, CCS polymers with either acidic or basic polar cores, and apolar arms were prepared via the reaction of dithiobenzoate terminated PSt chain transfer MIs with acrylic acid (AA) [73] or 4-vinylpyridine (4VP) [71] and a cross-linker in selected solvents. It was proposed that the polymerisation of AA and EGDMA with a PSt MI, in a non-solvent (benzene) for PAA, results in the formation of a PSt-*b*-P(AA-*co*-EDGMA) block copolymer, which at a critical chain length begins to aggregate and form micelles with P(AA-*co*-EDGMA) cores and PSt coronas (Scheme 7) [73]. Further polymerisation and cross-linking reactions occur in the core of the micelles to afford CCS polymers. When cyclohexene was employed as the solvent, gelation was observed as a result of aggregation of the block copolymers at much shorter P(AA-*co*-EGDMA) chain lengths, which leaves a large amount of monomers in solution that can readily undergo conventional polymerisation in the absence of the chain transfer agent. Support for the hypothesised polymerisation mechanism was demonstrated by monitoring the change in molecular weight and R_g of the polymer during the preparation of $PSt_{arm}P(4VP\text{-}co\text{-}DVB)_{core}$ CCS polymers [71]. Reaction of a dithiobenzoate terminated PSt chain transfer MI with 4VP and DVB in cyclohexene initially resulted in a slight increase in M_w that corresponded to the conversion of 4VP. However, after *ca.* 5 h the M_w and R_g increased sharply indicating aggregation of the copolymer to afford micelles. Interestingly, an increase in the DVB/MI molar ratio at a fixed 4VP/MI ratio resulted in a decrease in the conversion of 4VP and the R_g of the resulting CCS polymers.

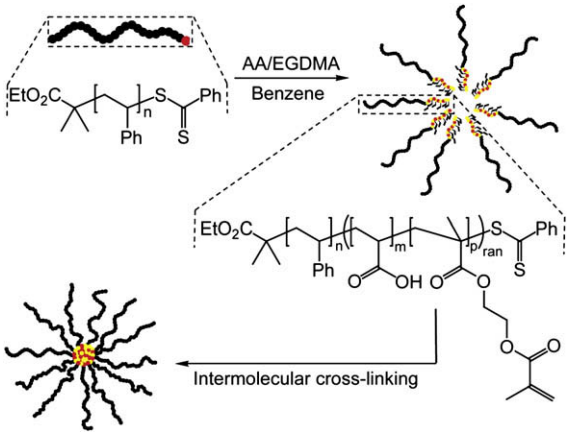

Scheme 7. Formation of $PSt_{arm}P(AA\text{-}co\text{-}EDGMA)_{core}$ CCS polymers via RAFT polymerisation and *in situ* micellation [73].

3.2. Structural diversity

In addition to the previously mentioned CCS polymers (Section 3.1) that possess homopolymeric arms, CRP and the arm-first technique also makes it possible to prepare a wide range of compositionally diverse and complex stars. For example, the preparation of CCS polymers using block copolymer MIs results in symmetrical stars with inner- and outer-shell morphologies (Fig. 4). Furthermore, careful selection of the polymeric blocks used in the arms enables the facile production of CCS polymers with amphiphilic characteristics or compartmentalised interior environments. Similarly, CCS polymer with gradient or random copolymer arms (Fig. 4) can be prepared using the corresponding MIs. Miktoarm (or asymmetrical) CCS polymers (Fig. 4) [35] possess molecular weight asymmetry (unequal arms) and/or chemical asymmetry (chemically different arms). Consequently, CCS polymers that have arms of similar chemical composition, but different end groups, can also be categorised as miktoarm stars.

3.2.1. CCS polymers with block copolymer morphology

CCS polymers with block and random arms comprised of *n*-butyl methacrylate (*n*-BMA) and MMA were prepared by Baek et al. via one-pot $ATRP_{(Ru)}$ using both EGDMA and BAM as cross-linkers [74]. When P^nBMA-*b*-PMMA, PMMA-*b*-P^nBMA and P(^{n}BMA-*co*-MMA) MIs of various DP were employed with EGDMA the yields (> 80%) of the resulting CCS polymers were high. However, attempts to employ the PMMA-*b*-P^nBMA MI with BAM did not yield the desired outcome as a result of the low reactivity of BAM with the *n*-BMA living end. In comparison, the formation of CCS polymers with the P(^{n}BMA-*co*-MMA) MI and BAM was successful despite the incompatibility issue mentioned previously. This was attributed to the addition of BAM before the complete consumption of MMA, which would have aided the formation of MMA terminated MIs suitable for reaction with the cross-linker BAM.

Similarly, Hawker and co-workers demonstrated that block copolymer CCS polymers could be easily prepared via the NMP of alkoxyamine functionalised block copolymer MIs using DVB in the presence of styrene as a spacer [75]. Starting from P^tBA-*b*-PSt, poly(*N*,*N*-dimethylacrylamide (PDMA))-*b*-PSt and poly(*N*-*iso*-propylacrylamide (PNIPAM))-*b*-PSt MIs the corresponding CCS polymers with apolar interior (inner shell) and polar exterior (outer shell) type morphologies were prepared efficiently (>72%).

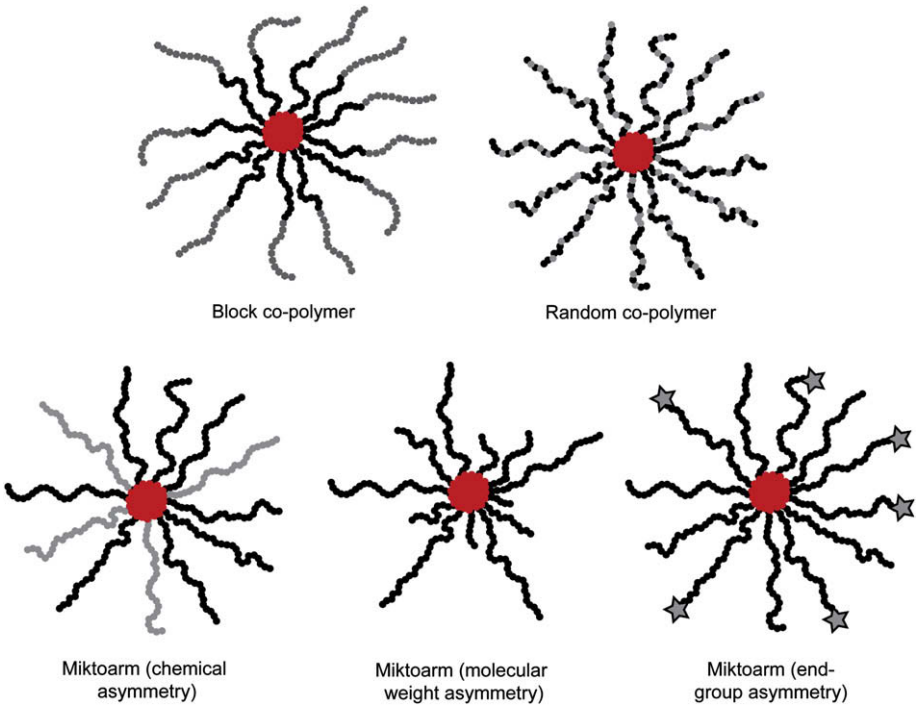

Fig. 4. Pictorial representation of CCS polymers with different types and combinations of arms.

Additionally, the inverted materials, with a polar interior and apolar exterior were also produced using PSt-*b*-P^{t}BA, PSt-*b*-PDMA, PSt-*b*-poly(4-vinylbenzoic acid (4VBA)), and PSt-*b*-poly(2-vinylpyridine (2VP)) MIs. Note that hydrolysis of the *t*-butyl ester groups present in the P^{t}BA containing stars was required to afford polar PAA functionalised CCS polymers. Furthermore, PSt-*b*-P(St-*co*-4VP) and PSt-*b*-P(St-*co*-maleimide) MIs were employed to produce CCS polymers with interior environments that could act as H-bond acceptors and acceptor–donor–acceptor H-bonding arrays, respectively. Following on from these studies water-soluble PEG-*b*-P(DMA-*co*-*N*-acryloxysuccinimide (NAS))$_{arm}$P(DMA-*co*-DVB)$_{core}$ and PEG-*b*-P(DMA-*co*-NAS)$_{arm}$P(DMA-*co*-ethylene glycol diacrylate (EGDA))$_{core}$ CCS polymers were prepared from alkoxyamine functionalised block copolymer MIs with different block sizes [76]. Subsequently, the activated esters of the NAS monomer units present in the inner shell of the CCS polymers were modified through reaction with a 1,4,7,10-tetraazacyclododecanetetraacetic acid (DOTA) derivative. The resulting DOTA functionalised stars were employed to chelate radioactive ^{64}Cu nuclei and their biodistribution and *in vivo* positron emission topography (PET) imaging was studied in relation to their structure. To determine the extent of DOTA conjugation to the CCS polymers as well as their availability to bind copper ions in aqueous solution, isotopic dilution assays (IDAs) were conducted. IDAs provided an estimate of between 10 and 36 DOTA groups per star, which is significantly lower than that determined by ^{1}H NMR (25–49 DOTA groups per star). The difference in results was attributed to shielding created by the outer shell of hydrated PEG, which results in only partial availability of the DOTA groups to chelate copper ions.

CCS polymers have also been prepared via the pre-assembly of amphiphilic block copolymers, functionalised with RAFT chain transfer agents, into micelles, which were subsequently cross-linked. For example, Zhang et al. prepared a range of amphiphilic poly(2-hydroxyethyl acrylate (HEA))-*b*-P^{n}BA copolymers, which formed micelles in methanol that could be cross-linked in the presence of 1,6-hexanediol diacrylate (HDA) and AIBN to afford soluble CCS polymers with narrow polydispersities (PDI = 1.12–1.24) [77]. Using a PHEA$_{260}$-*b*-P^{n}BA$_{75}$ chain transfer MI the effect of the HDA/MI molar ratio and MI concentration on the properties of the resulting CCS polymers was investigated. An increase in the HDA/MI molar ratio at a fixed MI concentration had negligible effect on the molecular weights and polydispersities of the CCS polymers. Likewise, an increase in the MI concentration had negligible effect up to a concentration of 2 mM, at which point multi-modal distributions were observed in the GPC RI traces and the yield of CCS polymer decreased significantly. In all cases a decrease in the hydrodynamic diameter (D_h) was observed upon cross-linking of the pre-assembled micelles. Dynamic light scattering (DLS) measurements of the micelles prior to cross-linking revealed that their D_h was dependent on the DP of both blocks of the copolymers and followed the general relationship $D_h \sim DP_{n\text{-}BA}^{1.17}.DP_{HEA}^{0.57}$. Lu and co-workers also prepared CCS polymers with block copolymer arms via the cross-linking of self-assembled micelles composed of RAFT chain transfer functionalised PNIPAM-*b*-PST MIs in water, using *N*,*N*-methylene bisacrylamide as the cross-linker in the presence of ammonium persulfate [78].

Similarly, Hales et al. prepared CCS polymers via the self-assembly of amphiphilic poly(lactic acid (LA))-*b*-PNIPAM chain transfer MIs in aqueous solution and found that the size of the micelles was dependent on the ratio of both blocks and the DP of each block [79]. An increase in the DP of either block or the overall molecular weight of the block copolymer resulted in an increase in the D_h of the micelles. Cross-linking of the micelle prepared from a PLA$_{60}$-*b*-PNIPAM$_{40}$ block copolymer was performed in methanol using HDA as the cross-linker in the presence of AIBN (Scheme 8). As a result of the location of the trithiocarbonate group between the two blocks, cross-linking resulted in the formation of a CCS polymer with a cross-linked layer between the core and the outer shell. DLS analysis of the CCS polymer in methanol revealed an increase in the average diameter, relative to the un-cross-linked micelle. Given the thermoresponsive behaviour of PNIPAM the lower critical solution temperature (LCST) of the block copolymers and CCS polymers was investigated via turbidity and light scattering measurements in aqueous solution. Whereas turbidity and

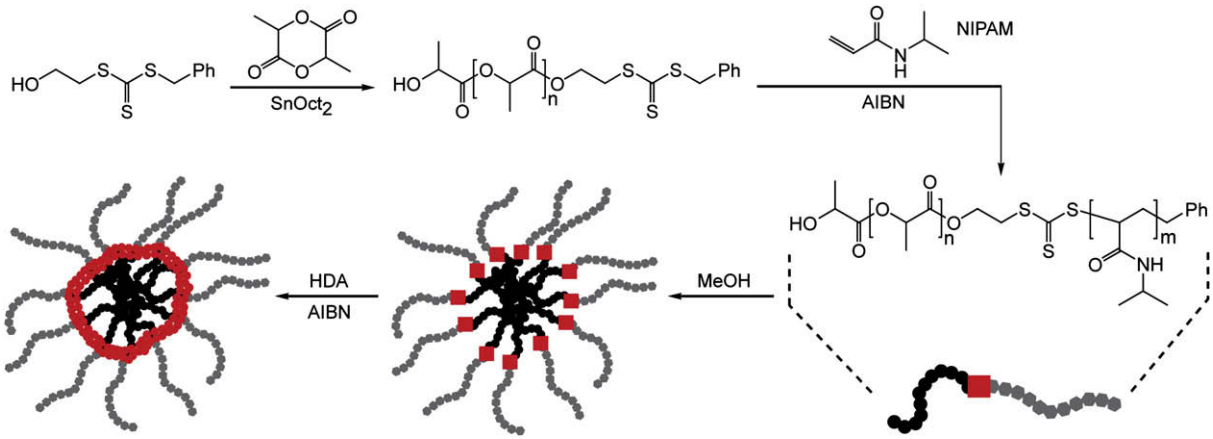

Scheme 8. Synthesis of PNIPAM-*b*-PLA CCS polymers with cross-linked layer between the core and the outer shell [79].

light scattering analysis of the CCS polymers yielded approximately the same LCSTs and rate of phase transition (~0.5 K), the block copolymers exhibited a very slow rate of transition (4–10 K), which was attributed to incomplete phase separation.

PCL-*b*-PMMA CCS polymers were prepared through a combination of $ATRP_{(Cu)}$ and ROP, and subsequently modified to manipulate the size and chemical composition of the shell structure [80]. For example, the outer PCL shell of a CCS polymer ($M_{n(MALLS)} = 226.0$ kDa, PDI = 1.18, $f \approx 7$) was hydrolysed to afford the corresponding PMMA star ($M_{n(MALLS)} = 207.0$ kDa), which was accompanied by a reduction in the D_h and molecular weight that was consistent with the theoretical removal of the PCL shell. This unique approach not only allowed for modification of the coronal properties, but also enabled access to CCS polymers with a few short arms, which would have been difficult to achieve via a direct synthetic approach. Furthermore, a PCL-*b*-PSt_{arm}PEGDMA$_{core}$ CCS polymer ($M_{n(MALLS)} = 544.4$ kDa, PDI = 1.25, $f \approx 20$) was prepared using a hydroxyl surface functionalised PSt_{arm}-$PEGDMA_{core}$ star ($M_{n(MALLS)} = 265.7$ kDa, PDI = 1.16, $f \approx 20$) as a MI for the ROP of ε-caprolactone. Based on the increase in molecular weight of the CCS polymer and the assumption that the initiation efficiency of the hydroxyl groups was 100%, the theoretical M_n of the arms was calculated to have increased from 7.7 to 21.4 kDa. Hydrolysis of the outer PCL shell resulted in the recovery of the original PSt CCS polymer ($M_{n(MALLS)} = 277.8$ kDa, PDI = 1.21, $f \approx 20$). Post-synthetic chain extension of the CCS polymer arms provides a simplistic route to prepare CCS polymers with many large arms, which are traditionally difficult to synthesis via a direct synthetic approach as the number of arms incorporated decreases as the arm molecular weight increases. Unfortunately, the initiation efficiency of the hydroxyl surface groups could not be determined, thus it was not evident if all the arms had been equally extended.

3.2.2. Miktoarm CCS polymers

Miktoarm CCS polymers have been prepared via CRP using two synthetic strategies, namely the 'in–out' method and a multiple MI approach. The 'in–out' method has been successful in preparing CCS polymers containing two kinds or arms with different chemical compositions and initially involves the formation of a symmetrical CCS polymer, which then acts as a multifunctional initiator for the subsequent growth of the second generation of arms. Noteworthy is the fact that as a result of the sterically congested core, initiation efficiency of the second generation of arms is reduced leading to miktoarm CCS polymers with fewer second generation arms relative to the first generation. Comparatively, miktoarm CCS polymers can be prepared with relative ease using a combination of MIs or MMs with different chemical compositions in a single reaction.

3.2.2.1. 'In–out' approach. Amphiphilic $PEG_{arm}PSt_{arm}$ miktoarm CCS polymers ($M_{n(CC)} = 69.1$ kDa, PDI = 1.22), which displayed micelle formation in water/THF solutions, were prepared via $ATRP_{(Cu)}$ of styrene from a PEG CCS polymer ($M_{n(CC)} = 42.6$ kDa, PDI = 1.12) [65]. From ^{1}H NMR spectroscopic analysis of the hetero-arm polymer it was deduced that the molar ratio of ethylene oxide to styrene repeat units was *ca.* 7:8, whereas elemental analysis provided a ratio of 4:3, which was in good agreement with the conversion of styrene. The same group has also reported the preparation of $PCL_{arm}PSt_{arm}$ miktoarm CCS polymers using PCL star polymers with PDVB cores as multifunctional initiators for the $ATRP_{(Cu)}$ of styrene [81]. In order to prevent star–star coupling and gel formation during the formation of the PSt arms it was necessary to keep the conversion of styrene low (3%) and at these conversions kinetic studies demonstrated that the styrene conversion displayed first-order kinetics, indicating that radical termination was negligible. Determination of the weight fraction of caprolactone units in the hetero-arm stars by ^{1}H NMR spectroscopy and elemental analysis was in good agreement and provided molar ratios of styrene/caprolactone units varying between 1.2 and 2.9. Presuming that the number of PSt arms was the same as PCL arms (i.e. all initiating sites initiated the polymerisation of styrene) it was estimated that the DP of the PSt arms was between 50 and 138.

To study the initiation efficiency of the initiating sites, present in the cores of CCS polymers, for the growth of a second generation of arms, Gao et al. prepared CCS polymers using the cleavable cross-linker, bis(2-methacryloyloxyethyl)disulfide **18** (SS) (Scheme 9) [82]. $ATRP_{(Cu)}$ of a PMMA MI and the disulfide **18** yielded the $PMMA_{arm}PSS_{core}$ CCS polymer **P2** ($M_{p(MALLS)} = 896.0$ kDa, PDI = 5.55, $f = 47$) that was completely cleaved into linear PMMA-*b*-PSH block copolymers (where SH represents the cleaved cross-linker **18**) upon the addition of tributyl phosphine. Using the polymer **P2** as a multifunctional initiator a second generation of arms was then grown with *n*-butyl acrylate (*n*-BA). Although a plot of $\ln([M]_0/[M])$ for *n*-BA conversion was initially linear, considerable deviation was observed after the first 5 h indicating intra- and intermolecular radical dimerisation, leading to a decrease in the number of living chains. The formation of star–star coupled products through intermolecular radical dimerisation was evident from GPC analysis and at longer reaction times gelation was also observed. Cleavage of the miktoarm CCS polymer produced a mixture of two types of block copolymers (PMMA-*b*-PSH and PMMA-*b*-PSH-*b*-PMMA), which confirmed that not all the initiating

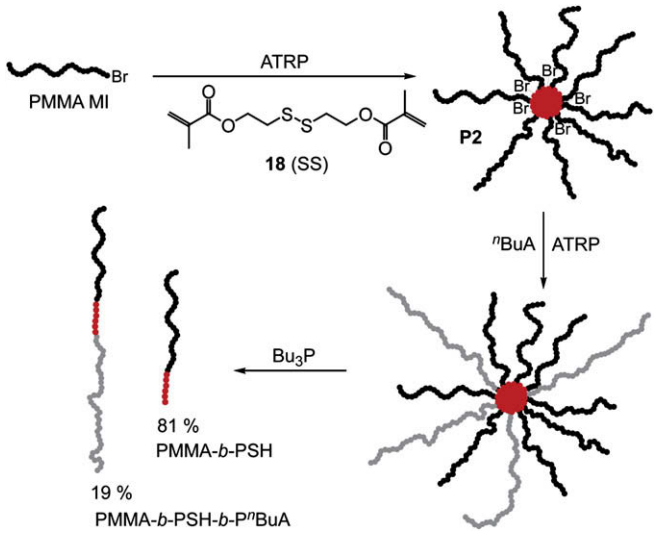

Scheme 9. Synthesis and cleavage of miktoarm CCS polymers prepared via $ATRP_{(Cu)}$ and the 'in–out' approach [82].

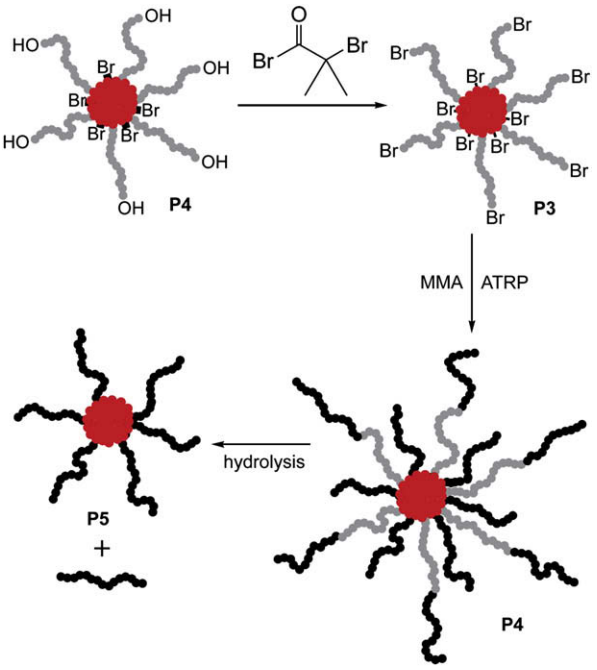

Scheme 10. Preparation of miktoarm CCS polymers with selectively degradable segments [80].

sites in the core of the homo-arm star **P2** initiated the polymerisation of *n*-BA. Deconvolution of the overlapping GPC RI responses for the di- and tri-block copolymers in combination with d*n*/d*c* values and weight fractions enabled the calculation of the ratio of the two copolymers, which corresponded to an initiation efficiency of 19% for the star **P2**. Knowing the initiation efficiency the number of second generation P^{n}BA arms and their DP was calculated as 9 (out of a potential of 47) and 389, respectively, using ^{1}H NMR spectroscopic analysis.

In a subsequent study the effect of several factors on the initiation efficiency of homo-arm CCS polymer multifunctional initiators was investigated using a kinetic method for the quantitative determination of the initiation efficiency [83]. Using P^{t}BA CCS polymers with various arm lengths and structural compactness values it was found that their initiation efficiency decreased with increasing arm DP and structural compactness. Given that longer arms and a denser star structure hinder access to the initiating sites it is unsurprising that the highest initiation efficiencies (54%) were obtained with stars that possessed short arms and low compactness values. The chemical compatibility of the first and second generation arms was also found to have a significant effect on the initiation efficiency. When the second generation was of the same chemical composition as the first P^{t}BA then the multifunctional initiator star had its highest initiation efficiency (33%), whereas the application of *n*-BA and methyl acrylate (MA) as monomers for the second generation led to a decrease in the initiation efficiency (30 and 23%, respectively). In contrast, when styrene was employed to prepare the second generation of arms the initiation efficiency dropped significantly (11%), highlighting the effect caused by the difference in chemical composition between the first and second generation arms.

The alkylbromide surface and core functionalised $PCL_{arm}PEGDMA_{core}$ CCS polymer **P3** ($M_{n(MALLS)} = 152.3$ kDa, PDI = 1.18, $f \approx 19$) were employed to prepare a miktoarm CCS polymer **P4** ($M_{n(MALLS)} = 514.6$ kDa, PDI = 1.29) (Scheme 10) comprised of both PMMA and PMMA-*b*-PCL arms that originated from the initiation of MMA from core and peripheral groups (on the pre-existing arms), respectively [80]. Hydrolysis of the inner PCL shell resulted in the recovery of CCS polymer **P5** ($M_{n(MALLS)} = 373.4$ kDa, PDI = 1.21) with PMMA arms originating from the core isolated initiating sites and linear PMMA that had been chain extended from the peripheral initiating sites. Given the known mass of the core and observed change in molecular weight upon degradation of the PCL segments, it was calculated that 83.7% of the total extended mass of the miktoarm CCS polymer **P4** resulted from core-initiated PMMA, whilst the other 16.3% was attributed to PMMA chain extension initiated from the arms. Therefore, the theoretical initiation efficiency of the core and peripheral sites was estimated to be 21% and 4%, respectively. These results suggest that initiation from the core was more easily achieved than initiation from the arms, which is unexpected given the steric congestion present within the cross-linked core. The observed trend was attributed to the high concentration of propagating radicals at the surface of the CCS polymer, which resulted in a higher rate of radical termination, as implied by the tendency of rapid gelation to occur during these reactions.

3.2.2.2. Multi-macroinitiator approach. The preparation of selectively degradable $PCL_{arm}PMMA_{arm}$ miktoarm CCS polymers was achieved by $ATRP_{(Cu)}$ of PMMA ($M_{n(MALLS)} = 7.5$ kDa, PDI = 1.08) and alkyl halide functionalised PCL ($M_{n(MALLS)} = 2.3$ kDa, PDI = 1.05) MIs in a 1:1 ratio using EGDMA as the cross-linker [84]. ^{1}H NMR spectroscopic analysis of the CCS polymer ($M_{n(MALLS)} = 559.6$ kDa, PDI = 1.24, $f \approx 53$) revealed a molar ratio of PCL:PMMA arms of 13:5, indicating that the relative reactivity of the MIs was dependent of their molecular weight, with smaller MIs being incorporated more readily. Acid-catalysed hydrolysis of PCL arms yielded a CCS polymer with a $M_{n(MALLS)}$ of 460.8 kD, which compared well with the theoretical M_n (472.5 kDa).

Recently, Matyjaszewski and co-workers have prepared a series of miktoarm star polymers containing two or more different combinations of arms via the $ATRP_{(Cu)}$ of DVB and MIs with different chemical compositions, but similar reactivity [85]. To demonstrate the application of the MI approach a $PMA_{arm}P^nBA_{arm}$ CCS polymer was firstly prepared by the reaction of equimolar amounts of PMA and P^{n}BA MIs of similar DP. ^{1}H NMR spectroscopic analysis revealed that the molar fraction of PMA to P^{n}BA arms in the fractionated CCS polymers was 0.52/0.48, which corresponded closely with the initial 0.50/0.50 molar ratio employed.

To confirm that the isolated CCS polymer was in fact a miktoarm star and not a mixture of two homo-arm stars the polymer was characterised by liquid chromatography under the critical conditions of PMA homopolymers, using normal phase silica columns as the stationary phase. Given that the elution volume of PMA containing copolymers was solely determined by the molecular weight of the other polymeric segments it was found that the elution volume of the $PMA_{arm}P^nBA_{arm}$ CCS polymer was less than that for a PMA star, yet higher than that for a P^nBA star, thus indicating that it was a miktoarm CCS polymer. Furthermore, by changing the molar ratio of the PMA and P^nBA MIs employed miktoarm CCS polymers with different arm compositions could be produced. The versatility of this innovative method was further illustrated by the preparation of a series of miktoarm CCS polymers with two types of arms with different compositions and molecular weights from various equimolar combinations of MIs. Moreover, elaboration of this method enabled the preparation of a miktoarm CCS polymer with five types of arms derived from the one-pot reaction of PEG, PSt, P^nBA, PMA and P^tBA MIs (Scheme 11). In all cases ^1H NMR spectroscopic analysis revealed that the arm compositions in the fractionated CCS polymers were always in good agreement with the initial composition of the MIs employed. Most recently, combinations of both MIs and MMs have been employed to prepare miktoarm CCS polymers [86].

3.3. CCS polymer morphology

CCS polymers, as with all star polymers, exhibit a gradient structure from the centre of the star to the outer shell with respect to the segment density of the arms [87–89]. The Daoud and Cotton model explains this by the division of the structure into three regions: a central core, a shell with semi-dilute density in which the arms have unperturbed chain conformation and an outer shell in which the arms of the star assume a self-avoiding conformation [90]. The major differentiating factor between CCS polymers and star polymers is the size and structure of the core. Whereas star polymers possess discrete and well-defined core moieties of relatively small molecular weight compared to the overall macromolecule molecular weight, CCS polymers have significantly sized cores that generally contribute 10–30% of the overall molecular weight. Therefore, it is evident that the cores of CCS polymers provide a unique environment, which has been exploited for various applications ranging from nanoparticle formation to encapsulation and storage of guest molecules. Furthermore, the highly cross-linked nature of the CCS polymer core reduces its flexibility and deformability, whilst conventional star cores are relatively mobile. The size and reduced mobility of the core can also affect the physical properties of CCS polymers as demonstrated by rheological studies [91] (Section 5.5), which highlight differences with star polymers that have relatively small cores.

3.3.1. Morphological characterisation

The size determination of CCS polymers is commonly conducted by light scattering techniques (MALLS, DLS and static light scattering (SLS)), however, more recently these results have been complemented by more direct imaging methods such as transmission electron microscopy (TEM) and atomic force microscopy (AFM). One of the first comparisons of CCS polymer dimensions obtained from light scattering and those from TEM were reported by Gurr et al. [92]. Whereas the R_g of a $PMMA_{arm}EGDMA_{core}$ CCS polymer ($M_{w(UC)} = 1.1$ MDa, $f \approx 15$) was determined to be 24.1 nm by light scattering, subsequent zero-loss TEM images of the polymer revealed particles ranging in size from *ca.* 10 to 20 nm with a mean diameter of 15.4 nm. Contrast inverted TEM images of the CCS polymer embedded in a PSt matrix provided diameter values ranging from 18 to 30 nm. It is evident that the size discrepancy observed from the light scattering and TEM results reflects the difference in conformation of the CCS polymer in different chemical environments. In solution, the arms of the CCS polymer are solvated and therefore, occupy a relatively large excluded volume. In comparison, casting the CCS polymer from a solution onto TEM grid (solid state) results in the arms collapsing onto the outer surface of the core, in which case the particles appear smaller. Likewise, when the CCS polymers are embedded into PSt matrix the PMMA arms are expected to contract as a result of the thermodynamically poor environment.

Sawamoto and co-workers examined the shape and size of a $PMMA_{arm}PBAM_{core}$ CCS polymer ($M_{w(MALLS)} = 525.0$ kDa, PDI = 1.31, $f \approx 29$) in toluene via small-angle X-ray scattering (SAXS) analysis [63]. The obtained scattering profile was fitted by the form factor of a spherical core–shell model, which showed satisfactory agreement at the small-angle regions and led to radius values of 2.7 and 8.8 nm for the core (R_c) and CCS polymer (R_p), respectively. Given that the R_g value (6.8 nm) calculated from R_p was very similar to the R_g value (6.9 nm) obtained separately from a Guinier plot using the same data it was concluded that the CCS polymers are spherical in shape. The structural ordering of 80% charged $PAA_{arm}PDVB_{core}$ CCS polymers above the overlap threshold concentration (1.6 wt%) in aqueous solution was investigated via SAXS [28]. SAXS analysis revealed that the CCS polymers adopted a body-centred cubic lattice structure and the packing density increased with increasing polymer concentration (4.7–11.5 wt%), regardless of the arm number and DP. Given that the measured nearest-neighbour distance (D_0) was proportional to *ca.* −1/3 power of the polymer concentration, as expected for homogeneous systems, it was concluded that the spherical particles of star polymers lead to isotropic shrinkage with an increase in the polymer concentration as a result of the softness of the PAA CCS polymers.

Small-angle neutron scattering (SANS) has also been employed to study the morphology and interactions of $PMMA_{arm}PEGDMA_{core}$ CCS polymers via the measurement of the scattered intensity as a function of the scattering vector (q) (Fig. 5) [61]. Three different contrast matches (none, arms and core matched) were measured and model fitting studies were then conducted to elucidate the conformational information of the CCS polymer ($M_{w(UC)} = 1.2$ MDa, PDI = 1.50). The experimental data was fitted to an inverted real-space model that defined functions in reciprocal space, such as the form and structure factors. The parameters in the model were subsequently refined until the fits converged. From Fig. 5 it can be observed that their is good agreement between the global fit and experimental data for the core- (arms data) and none-contrast matched (particle data) curves, however, there was poor fitting for the arm-contrast matched (core data) curve at low q values.

The failure of the model to globally fit the data at low q for the core data was believed to result from several assumptions about the structure of both the core and the particles. For example, the core was treated as a hard sphere in the model, whereas a function that describes the core as having a Gaussian falloff, with a gradual transition of the interface between the core and the arms may provide a closer global fit. Calculation of the R_c and R_p from the data

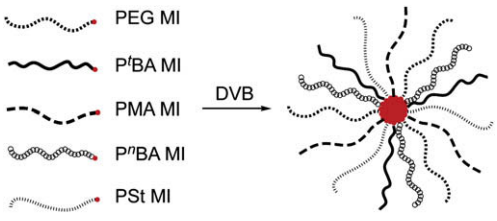

Scheme 11. Preparation of miktoarm CCS polymer via the $ATRP_{(Cu)}$ of DVB and MIs with different chemical compositions, but similar reactivity [85].

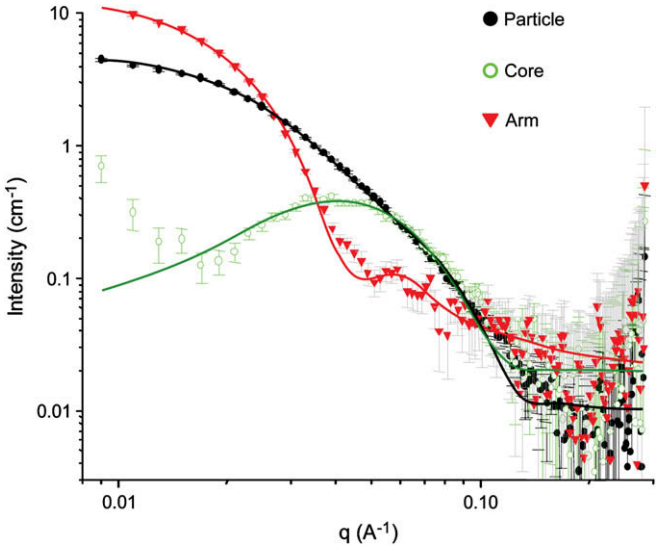

Fig. 5. SANS experimental results (data points) and global fits (solid lines) for arms (core-contrast matched), core (arm-contrast matched) and particle (none-contrast matched) of CCS polymer (2.5% w/v solution) [61].

provided values of 3.1 and 10.2 nm, respectively, which are on the same order of magnitude as those obtained from GPC MALLS analysis ($R_g = 16.2$ nm) and calculations of the minimum core size ($R_c = 4.8$ nm).

3.3.2. Core dimensions

In addition to R_c values determined from SAXS [63] and SANS [61] experiments (Section 3.3.1), the dimensions and characteristics of CCS polymer cores have been studied after chemical removal of the arms. To analyse the cores of $PEG_{arm}PDVB_{core}$ CCS polymers Du and Chen hydrolysed the ester group responsible for connection of the arms to the core and isolated the PDVB via fractional precipitation [65]. SEC of the PDVB revealed a $M_{n(CC)}$ of 7.6 kDa and PDI of 2.5, which was significantly higher than the PDI (1.12) for the CCS polymer. Given the reciprocal relationship that exists between apparent polydispersity and arm number it is evident that the greater number of low polydispersity arms a CCS polymer possesses the less significant the broad apparent PDI of the core becomes. Comparatively, similar results were obtained upon hydrolysis of a CCS polymer with PCL arms, which afforded a PDVB core ($M_{n(CC)} = 10.7$ kDa) with broad PDI of 5.6 [81].

Wiltshire and Qiao utilised DLS to analyse the core dimensions of CCS polymers after degradation of the arms [84]. CCS polymers with hydrolysable PCL arms were prepared via $ATRP_{(Cu)}$ using alkylbromide functionalised PCL MIs and either DVB or EGDMA as the cross-linker. The optimum conditions for the production of high molecular weight star polymers in good yields were found to be dependent on the cross-linker employed. For DVB a PCL concentration of 40 mM and cross-linker/PCL molar ratio of 15 were optimal, whereas for EGDMA a concentration of 5 mM and ratio of 25 yielded the best results. Acid-catalysed hydrolysis of CCS polymers with DVB or EGDMA cores ($M_{n(MALLS)} = 85.2$ kDa, PDI = 1.16, $f \approx 15$ and $M_{n(MALLS)} = 367.1$ kDa, PDI = 1.19, $f \approx 55$, respectively) resulted in the degradation of the PCL arms and enabled isolation of the cores, which possessed $M_{n(MALLS)}$ (43.7 and 215.7 kDa, respectively) closely matching the theoretically predicated molecular weights. DLS of the CCS polymers and their corresponding DVB or EGDMA cores after hydrolysis revealed a decrease in the diameter from 27 to 11 and 52 to 37 nm, respectively. Although the reduction in size in both cases was nearly identical it should be noted that the magnitude of the reduction is not solely dependent on the length of the removed arms, but also shrinkage of the exposed cross-linked cores as a result of a reduction in their solubility.

4. Functionalised CCS polymers

The versatility of the arm-first approach and tolerance of CRP techniques to a wide range of monomer families and functionalities have enabled highly functionalised CCS polymers to be developed in a controlled fashion with core, arm or peripheral functionality. However, when designing CCS polymers with complex functionalities the choice of CRP technique employed is of the upmost importance, as it has implications on the type of functional monomers and cross-linkers that can be employed [43]. The introduction of various functional groups into the core, arms or end groups of CCS polymers significantly enhances their potential application to polymer therapeutics, biodiagnosis, optical imaging, membranes, coatings, viscosity modifiers, catalysis, separation media, thin films and a variety of other advanced materials. Functionality can be imparted via several strategies: (i) the application of functionalised monomers for the preparation of MIs allows for the preparation of CCS polymers with arm functional groups (Scheme 12a); (ii) functionalised cross-linkers or functionalised monomers (as spacer groups) can be used to prepare core functionalised CCS polymers (Scheme 12b); (iii) functionalised initiators for the preparation of end-group functionalised MIs allow for the construction of peripherally functionalised CCS polymers (Scheme 12c); (iv) functionalised initiators can also be employed to produce core functionalised CCS polymers via the MM approach (Scheme 12d); (v) post-functionalisation can be achieved through the attachment of desired groups to complementary functionalities present in the preformed CCS polymer (Scheme 12e).

4.1. Peripheral functionality

The arm-first approach allows for the facile production of CCS polymers with peripheral functionality through the application of functional initiators for the preparation of the arms (MIs). For example, Zhang et al. synthesised a range of peripherally functionalised CCS polymers from α-functionalised P^{t}BA MIs via $ATRP_{(Cu)}$, which, in turn, were prepared from the corresponding alkylbromide initiators **19**–**24** (Fig. 6) [62]. Similarly, Baek et al. prepared a series of peripherally functionalised stars via $ATRP_{(Ru)}$, using amine, amide, ester and hydroxyl functionalised initiators **25**–**29** (Fig. 6) [47], although the polymerisation was found to be sensitive to the type of additive employed. When tri-*n*-butylamine was used as an additive for the one-pot polymerisation of MMA using initiators **25**–**28**, followed by the addition of EGDMA (added after MMA conversion reached 90%), the reaction proceeded smoothly with the formation of CCS polymers in good yields (75–91%) and with M_w values ranging between 346 and 1090 kDa. In comparison, when aluminium triisopropoxide was used as the additive under identical reaction conditions and using PMMA MIs prepared from the initiators **25** and **28** the resulting CCS polymer possessed broader polydispersities as a result of star-star coupling, whereas the MI derived from initiator **27** led to the formation of an insoluble gel as a result of exchange reactions between the hydroxyl end groups and the additive. The trends in molecular weight and yield of CCS polymers produced using α-functionalised PMMA prepared from the initiator **25** with different DPs and different molar ratios of EDGMA/PMMA [47] were found to be similar to those for PMMA without end-group functionality [46]. Bouilhac et al. synthesised methoxy and hydroxyl triethylene glycol surface functionalised $PSt_{arm}PDVB_{core}$ CCS polymers ($M_{w(MALLS)} = 447.0$ kDa, PDI = 1.60, $f \approx 110$ and $M_{w(MALLS)} = 331.0$ kDa, PDI = 1.30, $f \approx 64$, respectively) from

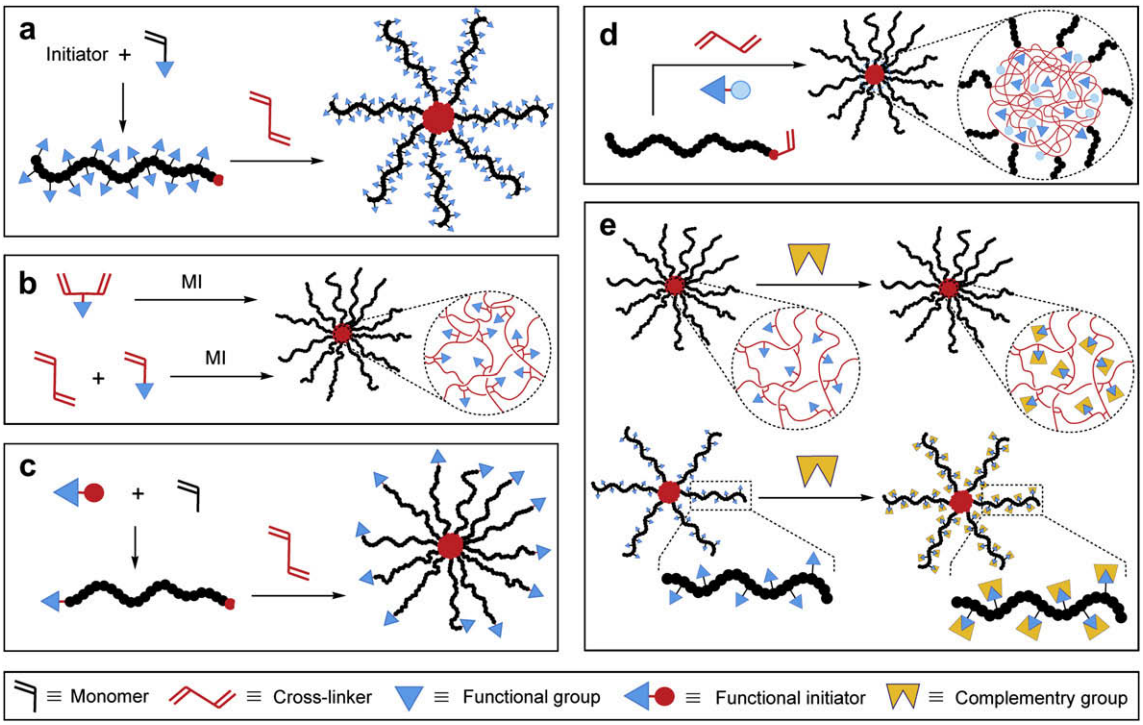

Scheme 12. Methods for the preparation of functionalised CCS polymers; (a) arm functionalised CCS polymers from functionalised MIs, (b) core functionalised CCS polymers from functionalised cross-linkers or monomers, (c) peripherally functionalised CCS polymers from end-group functionalised MIs, (d) core functionalised CCS polymers from functionalised initiators and MM approach; (e) core and arm functionalised CCS polymers via post-functionalisation.

α-functionalised PSt MIs derived from the alkylbromide initiators **30** and **31** (Fig. 6), respectively, using $ATRP_{(Cu)}$ [93].

Hawker and co-workers employed functionalised α-hydrido alkoxyamine-based initiators **32**–**35** (Fig. 7) to prepare peripherally functionalised CCS polymers via NMP [75]. Using a range of MIs derived from the alkoxyamine initiator **33**, stars comprised of either PSt, PDMA or PNIPAM arms and hydroxyl peripheral functionality were prepared via the cross-linking reaction with DVB and styrene. All of the CCS polymers possessed low polydispersities (PDI ≤ 1.26) and similar $M_{n(CC)}$ values (67–83 kDa). Furthermore, miktoarm CCS polymers were prepared by the copolymerisation of α-hydroxyl functionalised and unfunctionalised PDMA MIs in a ratio of 1:1. The accessibility of the peripheral hydroxyl groups was demonstrated by their quantitative post-functionalisation with the chromophore, 4-pyrenebutyryl chloride, which revealed that *ca.* 50% of the chain ends contained hydroxyl groups, in agreement with the molar ratio of the MIs employed in the synthetic strategy. $PSt_{arm}PDVB_{core}$ CCS polymers with glycoconjugated peripheral groups have been prepared via the NMP of PSt MIs derived from the TEMPO initiator **36** (Fig. 7) [94]. Calculations based upon SLS results revealed that the stars possessed 12–23 arms, which correlated exactly with the number of acetyl glucose end groups determined by specific rotation measurements. Subsequent deacetylation of the end groups afforded CCS polymers with glucose peripheral functionalities.

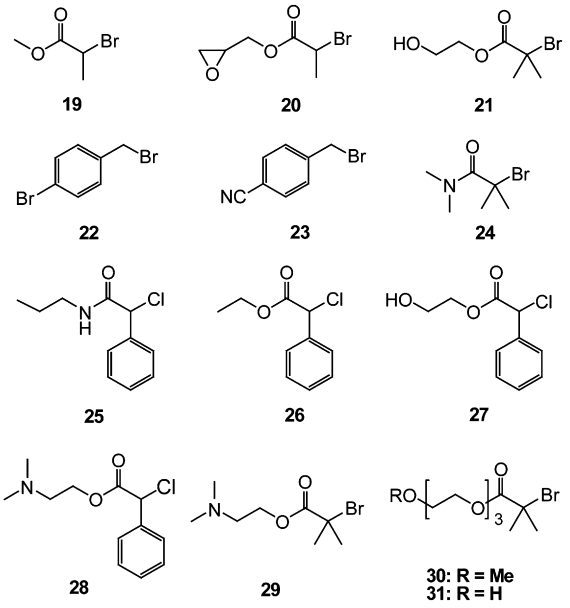

Fig. 6. ATRP initiators employed for the synthesis of peripherally functionalised CCS polymers [47,62,93].

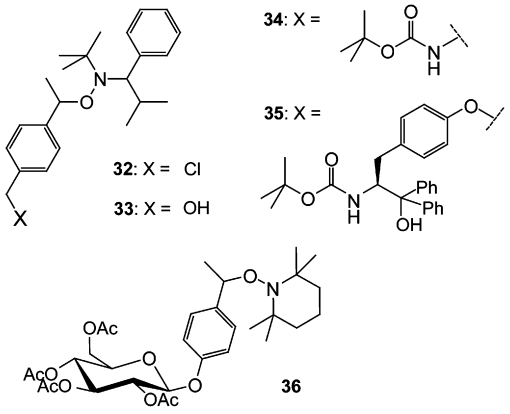

Fig. 7. NMP initiators employed for the synthesis of peripherally functionalised CCS polymers [75,94].

The major limitation associated with peripherally functionalised CCS polymers synthesised from initiators such as **19**–**36** is that the number of end-group functionalities on the star is equal to the *f*. Therefore, to overcome this restriction Connal et al. [95] employed dendronised initiators and $ATRP_{(Cu)}$ to firstly prepare dendron-*b*-PSt MIs, which were subsequently cross-linked using DVB to afford CCS polymers with significantly more peripheral groups than arms (Scheme 13). Dendron MIs (based upon the AB_2-type monomer, 2,2-bis(hydroxymethyl)propionic acid) of varying generation number (1st–5th) were prepared via the divergent growth approach and used to prepare block copolymer MI with different DPs, thus enabling the effect of dendron generation and MI DP on CCS polymer structure to be systemically studied. Keeping the DP of the PSt block on the dendron-*b*-PSt MI relatively constant (70–80) whilst increasing the dendron generation number leads to a slight decrease in the *f* of the resulting stars. More significant was the effect observed when the dendron generation number was kept constant (5th) and the DP of the PSt block was increased from 6 to 290. When a dendron-*b*-PSt MI with a DP of 6 was used stars with 37 arms were formed and the *f* was found to decrease exponentially as the DP was increased. Surprisingly, the presence of the highly branched fifth generation dendron attached to the end of the MI appeared to have little effect upon star formation given that polymers with large *f* could be prepared from sterically congested MIs with very low DPs. Likewise, Bosman et al. prepared dendron functionalised CCS polymers via the NMP of alkoxyamine terminated, fourth generation, benzyl ether dendron-*b*-PSt MIs with DVB [75] and found that CCS polymer formation was unaffected by the presence of the bulky dendritic end groups.

4.2. Core functionality

Both acid and base core functionalised CCS polymers **P6** and **P7** (Scheme 14) have been prepared by Fréchet and co-workers via the NMP of alkoxyamine terminated MIs with DVB, styrene and either phenyl 4-styrenesulfonate **37** or 4-(*N*-(2-(4-vinylbenzyloxy)ethyl)-*N*-methylamino)pyridine **38**, respectively [49]. Starting from a PSt MI ($M_{w(CC)} = 6.7$ kDa, PDI = 1.07) the acid CCS polymer **P6** ($M_{w(MALLS)} = 260.2$ kDa, PDI = 1.19, $f \approx 40$) was prepared with quantitative conversion of the MI and elemental analysis revealed *ca.* 100 sulfonic acid residues per macromolecule, which corresponds to 3–4 acidic groups per arm. Similarly, the basic CCS polymer **P7** ($M_{w(MALLS)} = 640.8$ kDa, PDI = 1.86, $f \approx 100$) was prepared from a PNIPAM MI ($M_{w(CC)} = 5.9$, PDI = 1.32) and determined by UV–visible spectroscopy to contain *ca.* 350 aminopyridine residues per macromolecule or 3–4 basic groups per arm.

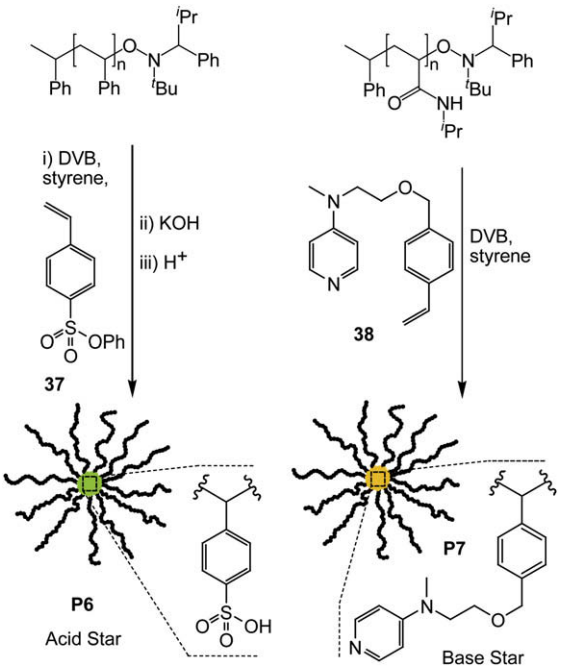

Scheme 14. Synthesis of acid and base core functionalised CCS polymers via NMP [49].

Several strategies have been employed to prepare fluorescently active CCS polymers, including the introduction of a fluorophore during core formation [96] and post-functionalisation. Gao et al. adopted a MM approach in which P^nBA containing an acrylate end group was copolymerised with DVB using the pyrene functionalised initiator **39** (Fig. 8) and $ATRP_{(Cu)}$ [97]. After a second addition of DVB and initiator **39** the weight fraction of pyrene in the fractionated CCS polymer ($M_{w(MALLS)} = 180.0$ kDa, PDI = 1.17, $f \approx 31$) was determined by UV–visible spectroscopy to be 0.016 g/g, which equates to *ca.* 80% incorporation. Similarly, amphiphilic CCS

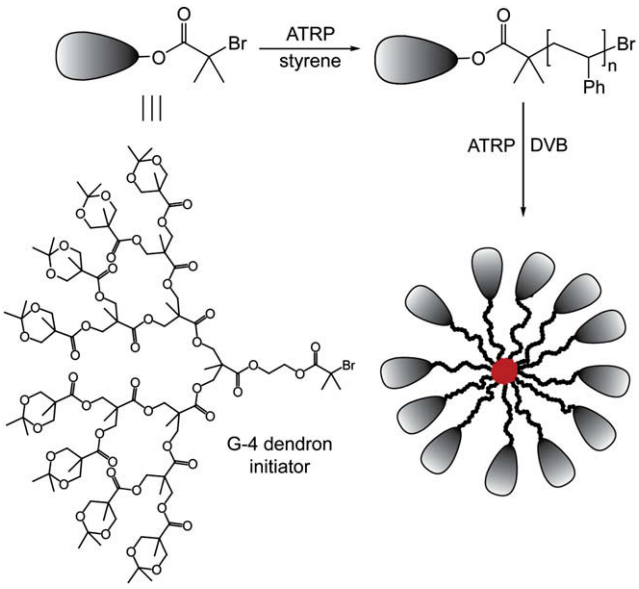

Scheme 13. Synthesis of dendron functionalised CCS polymer [95].

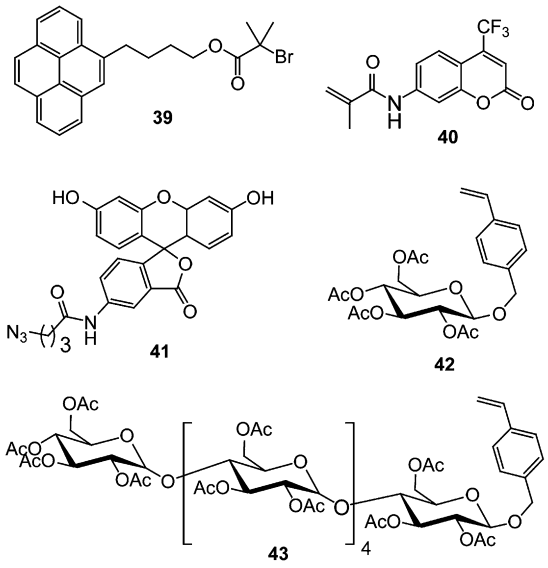

Fig. 8. Initiator and monomers used for the preparation of core functionalised CCS polymers [50,97–99].

polymers were prepared using PEG methyl ether methacrylate as the MM and EGDMA as the cross-linker. In this case, 74% of the pyrene initiator **39** was incorporated, which corresponded to an average of 13.5 pyrene groups per macromolecule. Spiniello et al. prepared a series of fluorescent CCS polymers with coumarin functionalised cores via the copolymerisation of DVB and the fluorescent monomer 7-[4-(trifluoromethyl)coumarin] methacrylamide **40** (Fig. 8), using a PMMA MI and $ATRP_{(Cu)}$ [50]. An increase in the amount of fluorescent monomer **40** from 2.5 to 12.5 mol% relative to DVB at a constant DVB/PMMA MI molar ratio resulted in a decrease in the $M_{w(MALLS)}$ (274.0–91.0 kDa), the f (20–7) and yield (83–44%) of the resulting CCS polymers. The % incorporation of fluorescent monomer **40** as determined by UV–visible spectroscopy varied from 68 to 88%, which corresponded to between 6 and 12 coumarin fluorophores per macromolecule. Surprisingly, the quantum yield of the fluorescent CCS polymer was found to increase as the amount of fluorophore covalently attached to the core increased. Given that fluorescent quenching might be expected at higher fluorophore concentrations this behaviour was attributed to changes in the composition of the micro-environment of the fluorophore. Fukukawa et al. prepared fluorescent star polymers via the cycloaddition of acetylene core functionalised CCS polymers with the azide functionalised fluorescein derivative **41** [98]. Initially, an alkoxyamine functionalised PEG-*b*-PDMA MI was reacted with the cross-linker EGDA in the presence of DMA and a trimethylsilane (TMS) protected acetylene acrylamide via NMP. After removal of the TMS groups the resulting CCS polymer ($M_{n(MALLS)} = 190.0$ kDa, $f \approx 30$), complete with core isolated acetylene functionalities, was reacted with the fluorescein **41** in the presence of $CuSO_4$ and sodium ascorbate. GPC coupled to an online photodiode array revealed the presence of the fluorescein within the core of the CCS polymers.

Glycoconjugated amphiphilic CCS polymers with either glucose or maltohexaose functionalised cores have been prepared via the NMP of TEMPO terminated PSt MI, using DVB as the cross-linker in the presence of acetylated vinylbenzyl-glucose **42** and -maltohexaose **43** derivatives (Fig. 8) [99]. An increase in the vinylbenzyl-saccharide/DVB molar ratio resulted in an increase in the molecular weight of the CCS polymers, whilst the yield was found to decrease. Incorporation of the saccharides into the cores was confirmed by characteristic methine and methylene proton resonances in the ^1H NMR spectra and measurement of the specific rotations, which increased as the initial vinylbenzyl-saccharide/DVB molar ratio used in the synthesis was increased. Deacetylation of the core-bound saccharides afforded amphiphilic CCS polymers that were capable of encapsulating water-soluble molecules.

Blencowe et al. prepared a series of Buckminsterfullerene C_{60} core functionalised CCS polymers via $ATRP_{(Cu)}$ of PMMA MI and EGDMA in the presence of pristine C_{60} [100]. The percentage incorporation (based upon the calculated and theoretical loadings) of the C_{60} into the CCS polymer was quantified via UV–visible spectroscopic analysis and decreased as the C_{60}/MI molar ratio was increased. An increase in the C_{60}/MI ratio from 0.02 to 0.5 resulted in an increase in the loading of C_{60}, whilst the M_w, R_g and the f of the CCS polymers remained relatively constant. A further increase in the ratio to 1 was found to hinder the CCS polymer formation reaction, resulting in a significant decrease in the M_w, yield and loading of C_{60}. Cyclic voltammetry of the C_{60} CCS polymer ($M_{w(MALLS)} = 372.0$ kDa, PDI = 1.15, $f \approx 25$) with a loading of 6.2 C_{60}/star revealed three reversible one electron reductions. However, compared to pristine C_{60} there was an anodic shift in the reduction potentials, which was attributed to the polar environment created by the polymer sheath of the core.

The incorporation of ligands into the cores of CCS polymers for the encapsulation of metals was investigated by Sawamoto and co-workers via $ATRP_{(Ru)}$ with the styrene functionalised phosphine derivative **44** (Scheme 15) [44,101]. The addition of cross-linker and diphenyl-4-styrylphosphine **44** to PMMA MIs (added after MMA conversion had reached 90%) resulted in the formation of CCS polymers with the spontaneous encapsulation of the ruthenium polymerisation catalyst. When the cross-linker (EGDMA or BAM)/MI molar ratio and MI DP were fixed at 10 or 100, respectively, whilst the phosphine monomer **44**/MI molar ratio was increased from 1.25 to 5 the incorporation of **44** remained high (89–100%), whereas the cross-linker conversion decreased (97–85% for EGDMA, 89–67% for BAM) [44]. In addition, as the **44**/PMMA molar ratio was increased the reaction time required to achieve a CCS polymer yield of >80% increased. Variation of the PMMA MI DP and cross-linker/MI molar ratio at a constant **44**/MI molar ratio resulted in similar trends to those observed in the absence of the phosphine monomer **44** [46,63]. The incorporation of ruthenium(II) into the cores of the CCS polymers was quantified by UV–visible spectroscopy and inductively coupled plasma atomic emission spectroscopy, which revealed an increase in the % incorporation relative to the amount of **44** employed in the polymer synthesis, implying that the phosphine functionalised cores was responsible for facilitating the inclusion via ligand exchange [44]. For the CCS polymer prepared using EGDMA and a **44**/MI molar ratio of 5 quantitative encapsulation of the ruthenium(II) was observed.

Most recently, Sawamoto and co-workers have extended this phosphine ligand mediated encapsulation methodology to the preparation of amphiphilic and thermosensitive ruthenium bearing CCS polymers [102]. As before [44,101], the one-pot $ATRP_{(Ru)}$ of poly(poly(ethylene glycol) methacrylate (PEGMA))-*b*-PMMA MI in conjunction with the phosphine derivative **44** (Scheme 15) and EGDMA resulted in the efficient formation of CCS polymers with the concurrent encapsulation of the ruthenium catalyst into the hydrophobic core [102]. As with the PMMA CCS polymers [44,101] the incorporation of ruthenium into the core of the amphiphilic stars was found to be dependent on the **44**/MI molar ratio employed and was similar regardless of the arm composition, indicating that the structure of the arms does not affect the ruthenium incorporation, nor is ruthenium encapsulated as a result of complexation with the PEG arms. In a similar fashion to the linear PPEGMA MI, the ruthenium functionalised PPEGMA-*b*-PMMA CCS polymers displayed thermosensitive properties when 2-propanol was used as a solvent, demonstrating that the hydrophobic interior is shielded from the external environment by the PEG-based arms. Above the upper critical solution temperature of 31 °C the CCS polymer was soluble, whereas below 31 °C the polymer precipitated out from solution.

A novel approach for the incorporation of functional groups into the core of CCS polymers was realised by Du and Chen using miktoarm CCS polymers composed of both PSt and degradable PCL arms (Scheme 16) [81]. Hydrolysis of the PCL arms afforded PSt stars with carboxylic acid functionalised PDVB cores, as confirmed by FT-IR spectroscopic analysis. The resulting amphiphilic star polymers with core carboxylated nano-environments were subsequently employed for the fabrication of lead sulfide particles via the reaction of lead acetate with the star followed by exposure to

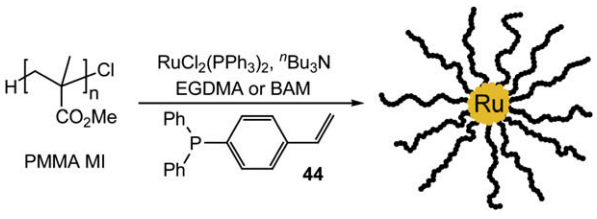

Scheme 15. Synthesis of phosphine core functionalised CCS polymer and *in situ* encapsulation of ruthenium [44,101].

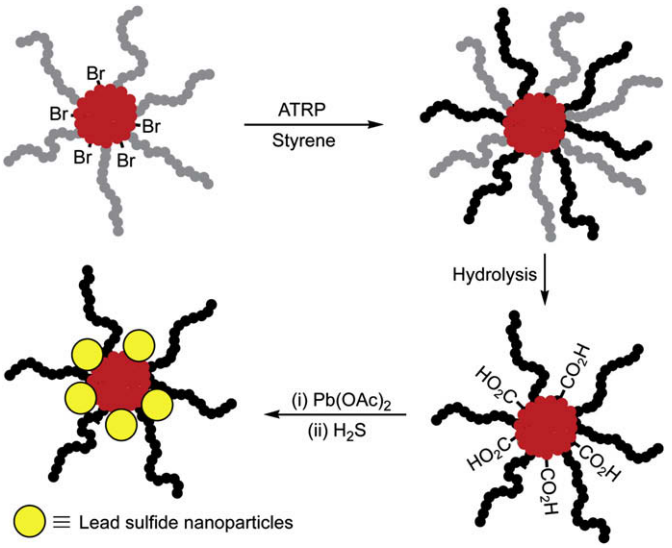

Scheme 16. Synthesis of $PSt_{arm}PDVB_{core}$ CCS polymers complete with internally compartmentalised lead sulfide nanoparticles [81].

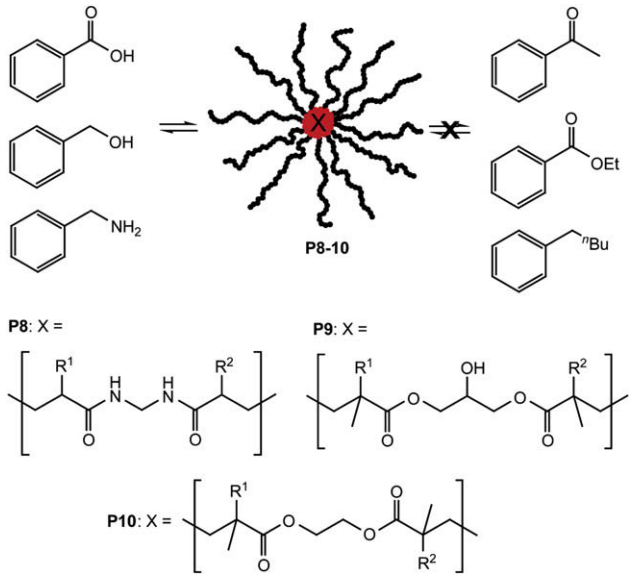

Scheme 17. Encapsulation of small molecules by core functionalised CCS polymers [103].

hydrogen sulphide to yield spherical lead sulfide nanoparticles having average diameters of 3 nm.

$PSt_{arm}PDVB_{core}$ CCS polymers prepared via RAFT polymerisation and with trithiocarbonate core isolated functionalities were employed to stabilise gold nanoparticles [59]. Initially, aminolysis of the trithiocarbonate with 1,2-ethylenediamine yielded a thiol functionalised core, which was used to bond $HAuCl_4$. Reduction of the core bound gold salt with $NaBH_4$ resulted in the formation of gold nanoparticles, which was accompanied by a change in colour to purple. TEM of the CCS polymer revealed dark gold particles with diameters in the range of 2–5 nm.

5. Properties and applications

5.1. Encapsulation

The encapsulation of hydrophilic molecules by peripheral and core glycoconjugated CCS polymers was investigated by Kakuchi and co-workers [94,99]. CCS polymers with glucose and maltohexaose functionalised cores successfully encapsulated methyl orange as demonstrated by UV–visible spectroscopy (methyl orange/CCS polymer = 11–39), which revealed that the amount of methyl orange incorporated dramatically increased as the hydrophilic saccharide component increased [99]. In comparison, the encapsulation of Rose Bengal by CCS polymers with peripheral glucose groups was less significant (Rose Bengal/CCS polymer = 0.70) [94]. Circular dichroism spectroscopy revealed characteristic Cotton effects in the vicinity of the absorption band of the encapsulated small hydrophilic molecules, which indicated their incorporation into the chiral saccharide regions of the CCS polymers [94,99].

Baek et al. tested a range of CCS polymers with different core functionalities for their ability to act as hosts for the selective interaction with small organic guest molecules [103] (Scheme 17). The interaction of protic and aprotic aromatic molecules with PMMA CCS polymers **P8**–**10**, with cores derived from the cross-linkers, **8**, 1,3-dimethacryloxypropan-2-ol and EGDMA (Fig. 3), respectively, was monitored by ^1H and ^{13}C NMR. For example, the successful interaction of benzoic acid with CCS polymer **P8** ([guest]/[core functional group in host] = 4) resulted in a broadening of the ^1H NMR aromatic resonances corresponding to benzoic acid as a result of a reduction of the thermal movement in the guest and a decrease in the ^{13}C NMR spin-lattice relaxation time of the *ortho* carbon of benzoic acid. Such interactions were absent for mixtures of benzoic acid with linear PMMA, PNIPAM and PMMA-*b*-PDMA, indicating that the amide functions within the core of **P8** were responsible for the host–guest interaction. Similarly, other protic guests such as benzylamine and benzylalcohol were found to interact with **P8**, whereas such interactions were absent for the aprotic acetophenone, ethyl benzoate and amylbenzene, implying that the host–guest interactions observed originate from the ability of the guest to form H-bonds with the amide core of **P8**. This was confirmed by reactions conducted with hydrogen bond breakers such as DMF or trifluoroacetic acid, which disrupted the host–guest interaction between **P8** and benzoic acid. Furthermore, benzoic acid was found to interact with CCS polymer **P9** as a result of the hydroxyl functionalities within the core, whereas the ester core of **P10** proved to be much less effective. Given the ability of the amide core of **P8** to successfully form H-bonds with protic guests it was demonstrated that in an equimolar mixture of benzoic acid and ethyl benzoate the CCS polymer **P8** selectively recognised and specifically formed interactions with only the protic guest. The hydrophilic core of **P8** was also found to be capable of the liquid–liquid extraction of the water-soluble dye, orange G, from an aqueous phase into an organic phase (deuterated chloroform) containing the CCS polymer. After mixing, phase separation revealed an intense red organic phase indicating the transfer of the dye (12.5% as determined from ^1H NMR), whereas in the absence of CCS polymer no transfer was observed.

The $P^tBMA_{arm}PEGDMA_{core}$ CCS polymer ($M_{w(MALLS)} = 236.0$ kDa, $f \approx 15$) with core isolated chiral groups based upon 1-amino-2,3-dihydro-1*H*-inden-2-ol was studied for its ability to recognise and interact with one of the enantiomers of a racemic mixture of 1,1′-bi(2-naphthol) ((*R*,*S*)-BINOL) [104]. The molecular recognition process was followed by ^1H NMR spectroscopic analysis, which revealed, upon the addition of the chiral CCS polymer, a splitting of the phenolic proton resonances corresponding to (*R*,*S*)-BINOL, thus indicating the ability of the chiral groups within the star core to specifically interact with one enantiomer.

CCS polymers with PSt-*b*-P(St-*co*-4VP) arms have been employed as supramolecular scaffolds, in which small molecules containing H-bond donors form host–guest complexes within the interior of the arms [75]. For example, the poorly toluene soluble

coumarin-3-carboxylic acid could be solubilised upon the addition of the PSt-*b*-P(St-*co*-4VP) star (Scheme 18a). FT-IR measurements revealed a shift of the O–H stretching band of the carboxylic acid to lower energies confirming that H-bonding was the driving force behind the formation of molecular complexes consisting of the acid and pyridine moieties within the star. The same star has also been used to encapsulate and solubilise zinc(II) protoporphyrin IX through a combination of metal ligand and H-bonding interactions as evidenced by ^{1}H NMR, UV–visible and fluorescence spectroscopies. The ability of the maleimide containing star, PSt-*b*-P(St-*co*-maleimide)-*b*-PSt$_{arm}$P(DVB-*co*-St)$_{core}$ to form multiple H-bonds with the complementary guest 2,6,-bis(acetylamine)pyridine (Scheme 18b) was assessed via NMR titrations and the association constant was found to be comparable to that of a small molecule model system. FT-IR analysis revealed the appearance of a new broad absorption band at lower energies, indicative of the formation of H-bonded complexes.

5.2. Catalysis

PMMA CCS polymers with triphenyl phosphine derivatives incorporated into the core were used for the *in situ* encapsulation of ruthenium(II) to afford catalytically active macromolecules [101]. The CCS polymers, which possessed various loadings of ruthenium (31–74 μmol Ru/g polymer) were employed for the catalytic oxidation of the alcohol, 1-phenylethanol to the ketone, acetophenone (Scheme 19). Although all of the CCS polymers induced the catalytic reaction, the activity was lower than that of $RuCl_2(PPh_3)_2$ and was found to decrease as the loading of ruthenium increased, implying that high catalyst loading adversely affects the activity.

The application of site isolation with regards to catalytically active polymers was elegantly demonstrated by Fréchet and co-workers who conducted a series of homogeneous one-pot reaction

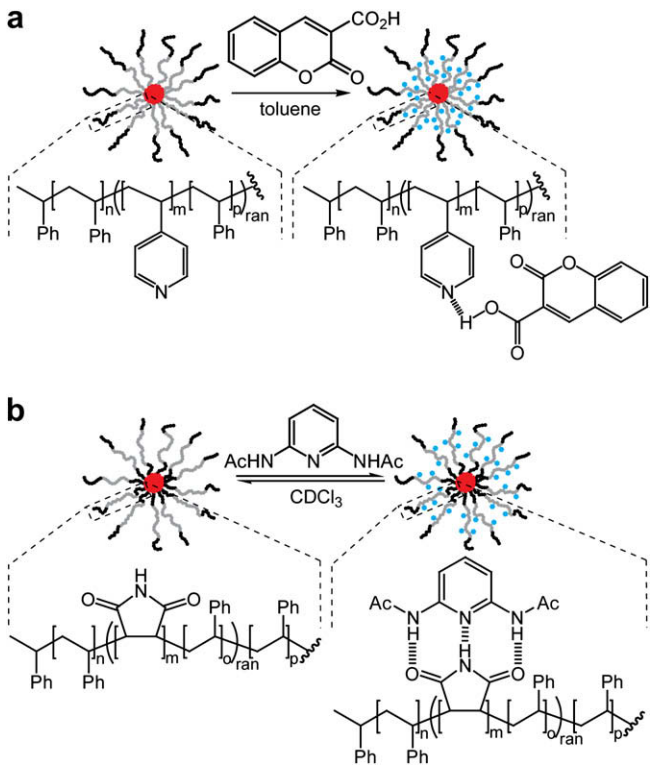

Scheme 18. Host-guest complexes of CCS polymers. Formation of H-bonding complexes between (a) PSt-*b*-P(St-*co*-4VP)$_{arm}$ stars and coumarin-3-carboxylic acid and (b) PSt-*b*-P(St-*co*-maleimide)-*b*-PSt$_{arm}$ stars and 2,6,-*bis*(acetylamine)pyridine [75].

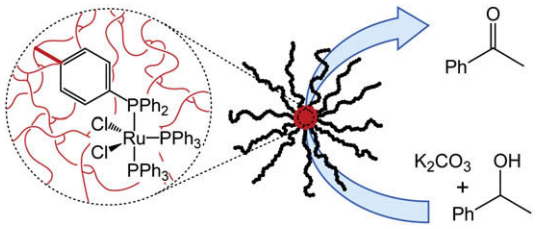

Scheme 19. Catalytic oxidation of 1-phenylethanol to acetophenone using PMMA$_{arm}$ EGDMA$_{core}$ CCS polymers with core isolated ruthenium(II) [101].

cascade employing both acidic and basic CCS polymers [49,105]. The isolation of the different catalytic groups to the cores of the CCS polymers suppressed mutual deactivation and enabled otherwise incompatible acid and base catalysed reactions to be conducted simultaneously. For example, in the presence of **P6** and **P7** (Scheme 14) the sequential acid-catalysed deprotection of 4-nitrobenzaldehyde dimethyl acetal **45** and amine-catalysed Baylis–Hillman reaction of 4-nitrobenzaldehyde **46** with methyl vinyl ketone proceeded smoothly with complete conversion of the acetal and a 65% yield of the Baylis–Hillman adduct **47** after 36 h (Scheme 20). In comparison, when either 4-(*N*,*N*-dimethylamino)pyridine (DMAP) or *p*-toluenesulfonic acid (PTSA) were used with **P6** or **P7**, respectively, only slight hydrolysis of the acetal was observed, indicating that DMAP and PTSA penetrate the core of the CCS polymers and deactivate the acidic and basic groups. Surprisingly, when a linear PSt-*b*-poly(styrenesulfonic acid) was employed in conjunction with the basic CCS polymer **P7** (or a base containing block copolymer with **P6**) the cascade reaction did not proceed, implying that the linear polymers can penetrate the corona of the CCS polymers. Thus, for the advantages of site isolation to be realised the catalysts must be restricted to the core of the CCS polymers.

CCS polymers with periphery located L-tyrosine based ligands were investigated as chiral auxiliaries for the catalytic alkylation of benzaldehyde with diethyl zinc [75]. In the presence of the star (0.05 mol%) quantitative formation of the enatiomeric alcohols, (*R*)- and (*S*)-1-phenylpropan-1-ol were observed with an enantiomeric excess of 71%, as compared to 18 and 77% for a peripherally substituted dendrimer analogue and low molecular PSt analogue, respectively. Whereas the CCS polymer and PSt analogue yielded similar results, the high molecular weight and branched nature of the star, would in theory, enable it to be easily recycled by the use of nanoseparation/filtration techniques.

PSt-*b*-P2VP CCS polymers have been employed as scaffolds for the preparation and stabilisation of palladium nanoparticles via the addition of $Pd(OAc)_2$ to the stars, followed by reduction of the bound palladium cations [75]. TEM analysis of the star-stabilised Pd-nanoparticles confirmed the formation of nanoparticles with diameters of 2–3 nm. The catalytic ability of the star-stabilised Pd-nanoparticles was demonstrated via the hydrogenation of cyclohexene and the Heck reaction of 1-bromo-4-nitrobenzene with *n*-BA. Whereas the catalytic hydrogenation proceeded with turnover frequencies comparable to other polymer stabilised

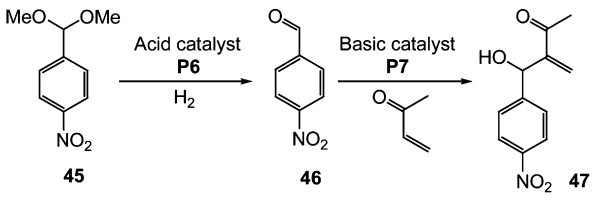

Scheme 20. Homogenous one-pot reaction cascade using both acidic and basic CCS polymers [49].

Pd-nanoparticles, the Heck reaction (in the presence of 0.5 mol% of stars) afforded the desired *trans*-cinnamate in almost quantitative yield. The steric stabilisation of the nanoparticles was demonstrated by the absence of palladium black formation. It was also demonstrated by precipitation that the catalytic stars could be recycled five times without any observable loss in performance. Furthermore, the PSt corona of the star polymers, surrounding the catalytically active interior, enabled the Heck reaction to be conducted in non-polar solvents as opposed to the traditional polar amidic solvents.

$PSt_{arm}PDVB_{core}$ CCS polymers with either hydroxyl or methoxy triethylene oxide peripheral groups were used to immobilise aluminic activators for the polymerisation of ethylene in the presence of the catalyst, 2,6-*bis*[1-2,6(diisopropylphenyl)imino]ethylpyridynyl iron dichloride [93]. The CCS polymers were initially mixed with a solution of methylaluminoxane (MAO), trimethylaluminium (TMA) or triisobutylaluminium (T^iBA) in order to immobilise the aluminic activators onto the star support. The required amount of iron catalyst was then introduced and the polymerisation of ethylene was performed under 1 bar of monomer pressure. For comparison, polymerisations were also conducted in the absence of the polymer support. In addition to the type of aluminic activator employed, the ratio of the activator to catalyst was also varied to investigate their influence on the catalytic activity and on the polyethylene (PE) characteristics. When T^iBA was employed as the activator the resulting PE exhibited a relatively narrow PDI in the presence and absence of the polymer support, although low catalytic activities were observed in both cases. With MAO as the activator, both unsupported and supported catalytic systems showed high activities, which were found to increase with the MAO/Fe ratio, however, examination of the bulk density and molecular weight characteristics of the PE revealed the beneficial effects of the CCS polymer support. For example, the bulk densities of PEs obtained in the absence of the polymer support ranged from 188 to 200 g L^{-1}, while the PEs prepared using the supported system had significantly larger values, ranging from 320 to 440 g L^{-1}. When the hydroxy terminated CCS polymer was employed as the support monomodal PE was obtained, whereas the unsupported system yielded bimodal PE. Similarly, if the polymerisation was carried out in the presence of either CCS polymer support, and using TMA as the activator, the resulting PEs were monomodal and had relatively narrow PDIs (Scheme 21). The ability of the CCS polymer supports to suppress the formation of bimodal PE was attributed to the immobilisation of the aluminic activators onto the polymer, which prevents the activators from acting as transfer agents.

5.3. Dewetting

The effect of dewetting in double-layer polymer assemblies comprising of linear PMMA bottom layers and linear PSt/$PMMA_{arm}PDVB_{core}$ CCS polymer blended top layers was investigated by Spontak and co-workers [106]. The resulting double-layer polymer assemblies were annealed at 180 °C and the dewetting process was monitored using time-resolved optical microscopy. When only PSt was used as the top layer the films spontaneously dewetted upon annealing to produce holes, with rims that contain dewetted material and that grow with time and eventually merge with neighbouring holes. In comparison, PSt blends containing 3 and 20 wt% of CCS polymer were found to dewet at a relatively slower rate, which was attributed to the migration of the stars to the PSt/PMMA interface where they act as surfactants, reducing the incompatibility between the two immiscible homopolymers. The topology of the PSt/PMMA interface for dewetted assemblies was analysed by AFM after selective removal of the PSt layer. Where holes had formed in the PSt blended (20 wt% CCS polymer) layer as a result of dewetting after 30 min the surface of the PMMA was rough with large CCS polymer aggregates, measuring on the order of 400–600 nm. In comparison, the interfacial area which remained in contact with the PSt/CCS polymer blend remained smooth. At longer annealing times the interfacial area that was present under these PSt/CCS polymer blend islands also underwent surface roughening to the extent that the areas under the islands and from the hole floors were indistinguishable. As a result of the high grafting density of arms on the CCS polymers and relatively high molecular weight of the PMMA substrate, an autophobic effect was observed, which prevents the CCS polymers at the PS/PMMA interface from sinking into the PMMA layer. Rather, the CCS polymers at the PSt/PMMA interface interact with one another via interpenetration of the arms, thus promoting the formation of aggregates as observed by AFM. The autophobicity-driven surface segregation and patterning of CCS polymers have subsequently been further elaborated upon to afford controllably patterned and reversibly switched substrates [107].

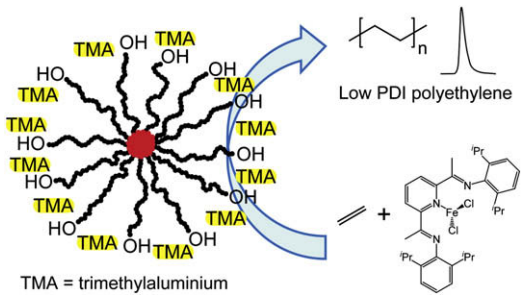

Scheme 21. Iron(II) catalysed polymerisation of ethylene using TMA immobilised on a $PSt_{arm}PDVB_{core}$ CCS polymer support as an activator [93].

5.4. Porous honeycomb assemblies

The first application of CCS polymers for the production of ordered honeycomb films was reported by Lord et al. [14]. Using optimised conditions a CCS polymer ($M_{w(CC)} = 49.9$ kDa, PDI = 6.30) was prepared by RAFT polymerisation of a dithiobenzoate terminated PSt MI with DVB in the presence of AIBN and samples were removed at various time intervals over a period of 48 h to assess their ability to form honeycomb structures. Scanning electron microscopy (SEM) images of the resulting films revealed that all of the polymers obtained at different reaction times with $M_{w(CC)}$ values ranging from 2.6 to 49.9 kDa formed porous films, although the pore size and distributions were found to vary considerably. For example, as the M_w increased up to 24.5 kDa there was a decrease in the average pore diameter, whereas further increases in M_w led to a large increase in pore diameter. Determination of Gini coefficient showed an inverted U-shape trend for the equality of pore size distribution with increasing M_w. Hence, material isolated at short and long reaction times produced films with favourable pore size equality, whereas those from intermediate times produced unfavourable conditions for equality between pore sizes. Complementary to this quantified virtual light scattering analysis revealed that the porous films constructed from material isolated at short and long reaction times produced good quality films in comparison to material isolated at intermediate times, although none of the films showed evidence of repeating angular alignment. These results indicated that the quality of the film is affected by the ratio of linear to CCS polymer components in the casting solution and that when a predominance of one component exits favourable conditions for honeycomb film formation are generated.

The purity, molecular weight and the *f* of $PMMA_{arm}EGDMA_{core}$ CCS polymers were found to play important roles in controlling the pore diameter and quality of honeycomb films prepared via the breath-figure technique [108]. SEM images of the films cast from

pure CCS polymer, isolated from fractionation of the crude polymerisation mixture (consisting of star and unconverted low molecular weight material), revealed a regular honeycomb structure with pore sizes and spacing consistent with the unfractionated sample, however, a higher degree of cracking was observed for the fractionated sample. It is well established that the relative humidity and flow rate of humid air used during the breath-figure film forming process have a significant effect on the honeycomb pore diameters, therefore these variables were kept constant to enable the effect of CCS polymer structure to be studied. Two series of CCS polymers with arm M_w values of 10 and 20 kDa and various overall M_w values and f were examined. For both series the average pore diameter decreased as the star M_w and the f were increased, with a larger dependence being observed for the 20 kDa arm series. The observed decreasing trend in pore size was attributed to the precipitation rate of the polymers, which was proposed to increase as a result of the increasing density (or the f) of the CCS polymers with M_w, given the relatively constant R_g values.

Connal et al. studied the effect of CCS polymer glass transition temperature (T_g) on the self-assembly of honeycomb films on planar and non-planar substrates [109,110]. CCS polymers comprised of PDMS, PEA, PMA, P^{t}BA or PMMA arms, with T_g values varying from −123 to 100 °C, were initially assessed for their ability to form porous honeycomb films on glass substrates via the breath-figure technique. SEM images of the resulting films revealed that all the CCS polymers formed honeycomb structures, although those with PEA and P^{t}BA arms formed slightly irregular patterns, whereas those with PMMA arms displayed regions of high order in addition to a high level of cracking throughout the film (Fig. 9a). The importance of the CCS polymer structure for the successful formation of honeycomb films was highlighted by the inability of the linear analogues of the star arms to form stable films. For example, linear PDMS, PEA, PMA and P^{t}BA either formed featureless transparent films or films with extremely disordered pores, which lost their features with time. Secondly, the stars were tested for their ability to form honeycomb structures on non-planar TEM grids placed on top of glass substrates. Whereas the PDMS, PEA, PMA and P^{t}BA CCS polymers formed porous honeycomb films that conformed to the non-planar TEM grid, the PMMA star did not contour to the grid and displayed a porous structure with extensive cracking. Of the CCS polymers that formed hierarchically ordered and porous films, those with PMA arms produced the most desirable structure, conforming to the TEM grid without the loss of underlying topography as a result of polymer relaxation (Fig. 9b). In addition, ordered honeycomb structures prepared on hexagonal and square TEM grids with various mesh sizes, using a PDMS star, were employed as soft-lithography templates to produce negative images by replica moulding [111]. The suitability of the PDMS star was further demonstrated through its ability to form honeycomb structures on inorganic particulate surfaces, including silica, glass micro-beads, kaolin, sodium chloride and sugar crystals [112] (Fig. 9c). In all cases the polymer successfully formed ordered porous films which contoured to the surface of the particles, regardless of its surface morphology. Furthermore, when honeycomb films were cast onto water-soluble particles it was found that the particles/templates could be removed by dissolution to afford micro-porous structures or porous pockets (Fig. 9d), thus demonstrating the flexibility of the regular porous films.

5.5. Rheological properties

The rheological behaviour of $PMMA_{arm}EGDMA_{core}$ CCS polymer ($M_{w(UC)} = 505.3$ kDa, PDI = 1.10, $f \approx 31$) solutions was examined initially via cone-and-plate rheometry [113]. Determination of the zero-shear viscosities (η_0) of different wt% solutions in xylene revealed an exponential increase as the concentration was increased from 30 to 60 wt%. The rheological properties of 80% charged $PAA_{arm}PDVB_{core}$ CCS polymers were investigated in aqueous solutions at polymer concentrations of 4.7, 8.0 and

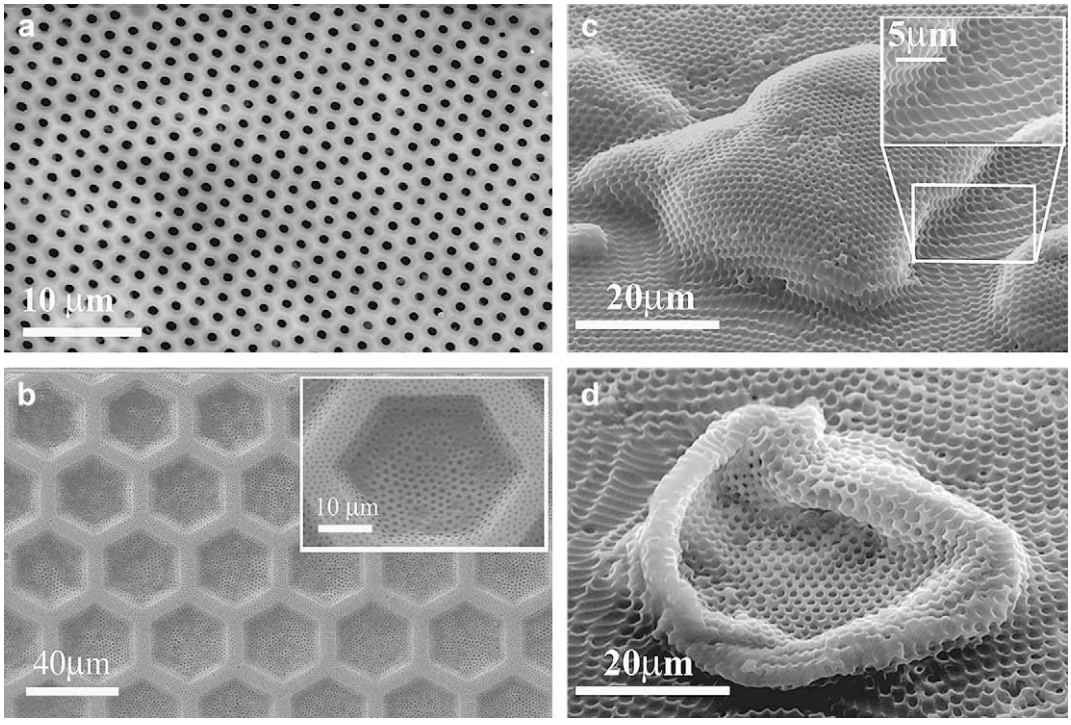

Fig. 9. SEM micrographs of honeycomb films: (a) PMMA CCS polymer on planar glass substrate [109], (b) PMA CCS polymer on non-planar hexagonal TEM grid [109], (c) PDMS CCS polymer on a sugar crystal [112], and (d) PDMS CCS polymer structure after dissolution of the sugar crystal [112]. Images (a) and (b) reprinted with permission from American Chemical Society (copyright 2008). Images (c) and (d) reproduced with permission from The Royal Society of Chemistry.

9.4 wt% via cone-and-plate rheometry [28]. Whereas 4.7 wt% polymer solutions were largely Newtonian in nature, higher wt% solutions were non-Newtonian and the 9.4 wt% solution possessed a yield stress of 190 Pa indicating the presence of solid-like structures. The viscoelastic behaviour of the CCS polymer solutions was determined by examination of the frequency dependence of the storage (G') and loss moduli (G''). For the 4.7 wt% polymer solution, G' and G'' exhibited typical behaviour for viscoelastic fluids. In comparison, for the 8.0 wt% polymer solution a crossover of G' and G'' was observed at a critical frequency, above which the system behaved as a solid. For the 9.4 wt% polymer solution, G' had a larger modulus than G'' across the frequency range studied. From these results it was concluded that the structural transition from a Maxwellian fluid of a weak liquid ordering structure to a macrolattice structure is by way of a sol–gel transition. Furthermore, the effective interaction between two star polyelectrolytes was compared with Lowen's prediction. This effective interaction, together with the G', was found to diverge at lower ϕ_{eff} values for polymers with greater f.

Goh et al. [91] studied the influence of star polymer ($M_{w(CCS)}$) and arm ($M_{w(arm)}$) molecular weight on the rheological properties of two series of $PMMA_{arm}PEGDMA_{core}$ CCS polymers: one with CCS polymers of equal $M_{w(arm)}$ and various $M_{w(CCS)}$ (**P11**–**P15**) and the other with equal $M_{w(CCS)}$ and different $M_{w(arm)}$ (**P12**, **P16** and **P17**). By plotting the relative viscosity data for the CCS polymers normalised with the particle hydrodynamic volume it was observed that the CCS polymers, like other star polymers, displayed a 'molecular softness' characteristic (Fig. 10), where the interpenetration and deformation of the 'soft' corona led to deviation from hard sphere behaviour and allowed higher effective volume fractions to be achieved. Stars **P12**, **P16** and **P17** with equal $M_{w(CCS)}$ displayed increasing molecular softness due to increasing $M_{w(arm)}$, whereas stars **P11**–**P15** with equivalent $M_{w(arm)}$ displayed similar molecular softness regardless of the f or $M_{w(CCS)}$. This latter phenomenon is unique to CCS polymers as other star polymers, such as chlorosilane-core stars or stars prepared via the core-first approach [114], display a strong variation of molecular softness with f. It was proposed that the different trends observed for the CCS polymers and star polymers resulted from the different core structures of the macromolecules, which in turn, can be attributed to the mechanisms of star formation via the arm-first and core-first synthetic approaches [91].

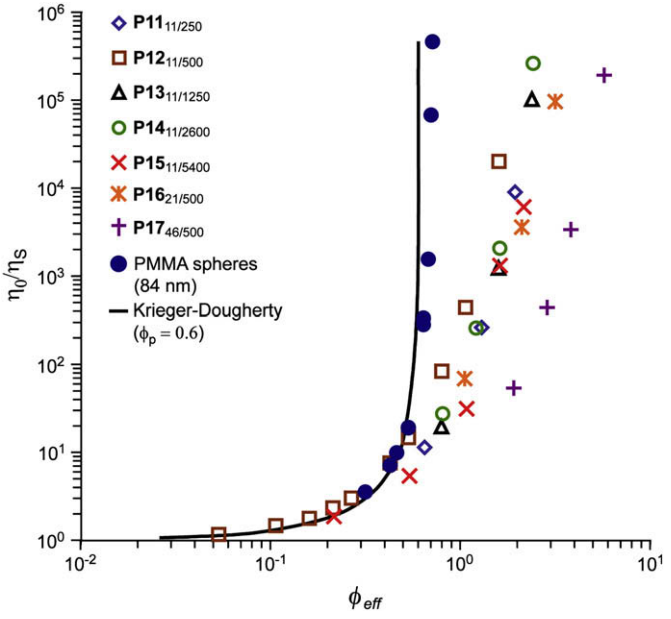

Fig. 10. The relative viscosities (η_0/η_s) for CCS polymer solutions as a function of the effective volume fraction (ϕ_{eff}). The molecular softness characteristic of CCS polymers is clearly observable when compared to PMMA spheres and the Krieger–Dougherty equation for colloidal particles [91].

For the CCS polymer series **P11**–**P15** ($M_{w(MALLS)} = 250$–5400 kDa, $f = 17$–360) the core molecular weight increased comparatively with the $M_{w(CCS)}$; thus the percentage contribution of the core (~25%) to the $M_{w(CCS)}$ remained relatively constant. Therefore, as f increases the size of the core also increases; thus, the segmental density remains relatively constant and the molecular softness for these CCS polymers is comparable. In contrast, star polymers with discrete, molecular cores display a strong relationship between molecular softness and f. This is due to the different arm conformations adopted depending on the degree of arm crowding. Low f star polymers have arms with approximately random coil conformations, but increasing f leads to crowding in close proximity to the core and the polymeric arms acquire a more stretched conformation. Ultimately, high f star polymers have rigid coronas consisting of highly stretched polymeric arms which display very little molecular softness; they behave like hard spheres.

5.6. Thermal properties

In general, CCS polymers display T_g values that correspond to the arms and are similar to linear polymers of the same composition. As one might expect from a cross-linked network, the core of CCS polymers display no T_g values as a result of their rigid structure and lack of mobility. For example, differential scanning calorimetry of CCS polymers comprised of PDMS, PEA, PMA, P^{t}BA or PMMA arms displayed single T_g values (−123, −30, 2, 48 and 100 °C, respectively) [109], which were in accordance with literature values for the corresponding linear analogues of the arms. Similarly, the T_g of a $PMMA_{arm}PDVB_{core}$ CCS polymer was reported to be comparable with that of a linear analogue of the arms [115]. In neither case were transitions observed for the core. The thermal degradation of a $PMMA_{arm}PDVB_{core}$ CCS polymer was investigated by Goh et al. using thermal gravimetric analysis [115]. Two major degradation events were observed at 405 and 460 °C and were attributed to PMMA random chain scission and PDVB degradation, respectively.

5.7. Polymer therapeutics

Highly branched macromolecular architectures including star polymers and dendrimers have attracted significant attention due to their potential in polymer therapeutics [116,117] and in particular, drug delivery [118]. For example, amphiphilic dendrimers with hydrophobic interiors and hydrophilic coronas have the capacity to accommodate hydrophobic drugs within their interior, providing a means to transport the payload through aqueous media to the desired physiological target [119]. The capacity of these macromolecules to solubilise hydrophobic drugs, target specific physiological sites and control the rate of drug release has enabled the development of drug delivery systems that can reduce dosage requirements through the targeted and controlled delivery of the payload to the desired site [116]. Given the core–shell type morphology and ease of functionalisation it is evident that CCS polymers have great potential in drug delivery and other therapeutic applications. However, to date very few studies have exploited CCS polymers for such applications [120]. Some preliminary studies have been focused on the development of degradable CCS polymers with the potential to control the rate of drug release relative to the degradation rate [16,80,84,121].

The biodistribution and PET imaging of PEG-*b*-P(DMA-*co*-DOTA)$_{arm}$P(DMA-*co*-DVB)$_{core}$ and PEG-*b*-P(DMA-*co*-DOTA)$_{arm}$P(DMA-

co-EGDA)$_{core}$ CCS polymers (Fig. 11), labelled with the radioactive medium lived positron emitter ^{64}Cu (5–10 mCi/mg star), were investigated by Hawker and co-workers *in vivo* [76]. Given that the major drawback with polymer therapeutics and nanoparticles is their fast elimination from the blood stream due to particle separation by the mononuclear phagocytic system (MPS), the DOTA inner-shell functionalised star polymers were examined for their *in vivo* blood retention and accumulation in the major MPS organs (liver and spleen) of rats. The blood retention and MPS uptake were found to be highly dependent on the DP of the PEG outer shell of the star polymers. For example, CCS polymers with 5 kDa PEG outer shells were still present 48 h after intravenous injections, whereas stars with 2 kDa PEG outer shell had completely cleared the system. In comparison, the CCS polymer size and core composition had negligible effect on the blood retention time, but a noticeable effect on the hepatic and splenic uptake, with smaller CCS polymers ($M_{w(MALLS)} = 201.0$ kDa, $f \approx 12$, $D_h = 33.7$ nm) or those with P(DMA-*co*-EGDA) cores accumulating slower than the larger ones ($M_{w(MALLS)} = 456.0$ kDa, $f \approx 10$, $D_h = 70.4$ nm) or those with P(DMA-*co*-DVB) cores. To determine the application of the CCS polymers for imaging of the circulatory system mice were administered with both the precursor ^{64}Cu-labelled block copolymer MIs and the corresponding star polymers and imaged by microPET Focus at selected times (1, 4 and 24 h), post-injection. The heart and major blood vessels of the mice injected with the CCS polymers were clearly visible at each time point, although the heart standardised uptake value decreased faster for the stars with 2 kDa PEG outer shell, confirming its faster blood clearance. The accumulation of CCS polymer in the MPS organs was also confirmed, with the liver being the most noticeable organ, especially at 4 and 24 h after administration. In comparison, the block copolymer arms displayed insignificant accumulation in the liver, heart and blood vessels, instead the kidney and bladder were the only visible organs due to fast urinary excretion.

5.8. Polyelectrolytes

Connal et al. synthesised a polyelectrolyte PAA$_{arm}$PDVB$_{core}$ CCS polymer ($M_{w(MALLS)} = 270.0$ kDa, PDI = 1.09, $f \approx 32$) via the acid hydrolysis of the corresponding P^{t}BA$_{arm}$PDVB$_{core}$ CCS polymer ($M_{w(MALLS)} = 397.0$ kDa, PDI = 1.12), previously prepared via ATRP$_{(Cu)}$ [122]. Acid–base titrations revealed that more than 90% of the *t*-butyl groups were successfully cleaved, which agreed well with the reduction in M_w observed from GPC analysis. The activity coefficient (α) and hence the degree of ionisation were calculated by pH titration experiments and the p$K_{a,app}$ of the PAA CCS polymer was determined to be 6.5. In comparison, the p$K_{a,app}$ value of linear PAA was reported to be 5.8. The observed disparity [123] results from the higher osmotic pressure inside the CCS polymer, which causes a partial reversal of ionisation, where there are less charged ions in the confined regions of the star. Subsequently, the D_h of the PAA CCS polymers at different degrees of ionisation was analysed via DLS. Starting from a star polymer solution at pH 11, the pH was gradually adjusted to 2 and then back again. At the initial high pH the acid groups were completely charged and as a result, the PAA arms are extended leading to a maximum in D_h (32 nm) of the CCS polymer. A decrease in the pH to 2 was accompanied by a decrease in the D_h to 23 nm, which was attributed to the coiled conformation of the PAA arms due to a decrease in the degree of ionisation. As the pH was increased again the D_h also increased, however, the maximum observed value was 27 nm. The difference in this value and the initial D_h results from the increase in salt concentration as the pH is changed, which causes screening of the charges on the PAA CCS polymer.

Similarly, Furukawa and Ishizu prepared polyelectrolyte PAA$_{arm}$PDVB$_{core}$ [28] and PMAA$_{arm}$PEGDMA$_{core}$ [124] CCS polymers from *t*-butyl derivatives and investigated their conformation as a function of pH and ionic strength. DLS analysis of dilute solutions of PAA and PMAA CCS polymers revealed that, like their *t*-butyl precursors, the translational diffusion coefficient ($D(c)$) as a function of polymer concentration remained relatively constant, implying that the majority of counterions are located within the star and aggregation as a result of the polyelectrolyte effect of interchain interaction is negligible. The dependence of the D_h of PMAA CCS polymers (p$K_a = 6.6$) was investigated as a function of the degree of ionisation, brought about by a change in pH [124]. It was determined that the D_h increases with increasing pH from 18.3 to 48.3 nm as a result of the osmotic pressure exerted by the counterions trapped within the arms (Scheme 22). Furthermore, the dependence of the D_h on the ionic strength of the solution was studied via the addition of NaCl. At low salt concentrations (10^{-6}–10^{-3} M) the D_h of the PMAA CCS polymers decreases gradually from 55.4 to 48.8 nm, whereas if the salt concentration ($>10^{-3}$ M) in the bulk of the solution sufficiently exceeds the intrinsic concentration of the counterions within the star the D_h decreased significantly. The large decrease in D_h at high salt concentrations was attributed to the contribution of both co-ions and counterions to participate in intramolecular screening, whereas at low salt concentrations, the screening is dominated by counterions [124]. More recently, polyelectrolytic CCS polymers have been employed in pH-switchable complexation with cationic block polyelectrolytes [125] and as pH-responsive nanoparticles [126]. In addition, there has also been the presentation of new scaling theories for solutions of star polyelectrolytes [127], which distinguish between two cases of counterion distribution around the arms and describe differences in the structure of the stars in the presence and absence of counterions condensed on the arms.

5.9. Multi-layer absorbed films

Polyelectrolyte CCS polymers have been employed in combination with linear poly(allylamine hydrochloride) (PAH) to produce pH-responsive multi-layer films [122]. Thin films were fabricated via the layer-by-layer deposition approach, in which alternating

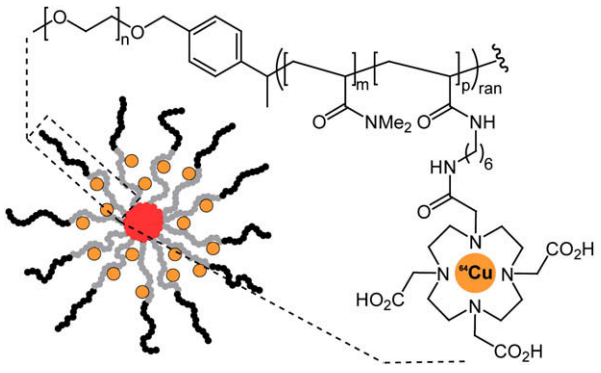

Fig. 11. Structure of PEG-*b*-P(DMA-*co*-DOTA) CCS polymers labelled with the radioactive medium lived positron emitter ^{64}Cu [76].

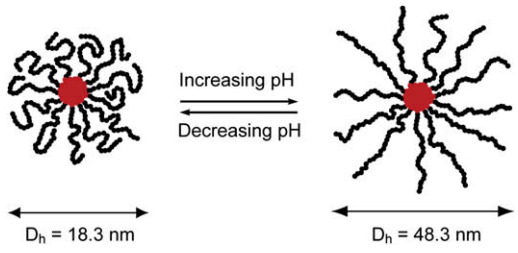

Scheme 22. Dependence of the D_h of PMAA$_{arm}$PEGDMA$_{core}$ CCS polymers as a function of the degree of ionisation, brought about by a change in pH [124].

adsorption of PAA CCS polymers and linear PAH was achieved through dip-coating at pH 7.5. The assembling process was followed by quartz crystal microbalance (QCM) measurements, which provide a value of 91 nm for the thickness of the film after 16 layers had been deposited. Furthermore, the QCM measurements revealed an exponential multi-layer growth profile, which was hypothesised to result from diffusion of the PAH chains, as diffusion of the PAA star was unlikely given its high molecular weight and globular structure. Subsequently, the pH-dependent surface morphology of a 17-layer PAA CCS polymer/PAH film assembled at pH 3.5/pH 7.5 and with the star as the outmost layer was examined by AFM. The film thickness as determined by AFM was 60 nm and exhibited a rough and porous surface. The film was then exposed to either pH 2 or pH 11 aqueous solutions. Fourier transform infrared (FT-IR) spectroscopic analysis of the films after treatment at pH 2 or pH 11 enabled determination of the proportion of protonated carboxylic acid groups (~85%) or ionised carboxylic acid groups (~85%), respectively. AFM images of the film after treatment at pH 2 revealed a phase separation-induced 'wormlike' surface structure comprised of grain domains, which was attributed to the highly coiled conformation of the PAA arms. In comparison, images of the film after treatment at pH 11 revealed a relatively smoother surface structure due to the extended conformation of the arms. To investigate the reversibility of the morphology transitions, the films were further exposed to the opposite pH conditions to which they had been exposed prior. Images of the film initially treated at pH 2 and subsequently exposed to pH 11 revealed that the wormlike surface was maintained whilst the grain domains became smooth. Images of the film initially treated at pH 11 and subsequently exposed to pH 2 were very similar to the film solely treated at pH 2, thus demonstrating the reversible pH behaviour of the film.

6. Summary

Given the significant body of work that has been conducted into CCS polymers it is evident that this is a very active area of polymer research, encompassing not just synthetic chemistry, but also the disciplines of physical chemistry, materials science and polymer therapeutics. Over the past decade considerable effort has been expended to optimise the controlled radical synthetic protocols required for the preparation of well-defined CCS polymers; thus laying the foundation for future advances and the development of increasingly more complex and sophisticated polymeric materials. It is only recently that the application of such intricate and functionally diverse CCS polymer architectures has started to be realised and it is foreseeable that in the not to distant future CCS polymers will play a major role in many advanced materials and technologies.

References

[1] Szwarc M. J Polym Sci Part A Polym Chem 1998;36:ix–xv.
[2] Hadjichristidis N, Iatrou H, Pitsikalis M, Mays J. Prog Polym Sci 2006; 31:1068–132.
[3] Zilliox J-G, Rempp P, Parrod J. J Polym Sci Part C 1968;22:145–56.
[4] (a) Sogah DY, Hertler WR, Webster OW. Polym Prepr Polym Div Am Chem Soc 1984;25(2):3;
(b) Simms JA, Spinelli HJ. J Coat Technol 1987;57:125.
[5] Webster OW. J Polym Sci Part A Polym Chem 2000;38:2855–60.
[6] Bazan GC, Schrock RR. Macromolecules 1991;24:817–23.
[7] Kanaoka S, Sawamoto M, Higashimura T. Macromolecules 1991;24: 2309–13.
[8] (a) Solomon DH, Rizzardo E, Cacioli P. US Patent 4,581,429; 1986;
(b) Georges MK, Veregin RPN, Kazmaier PM, Hamer GK. Macromolecules 1993;26:2987–8.
[9] (a) Wang JS, Matyjaszewski K. J Am Chem Soc 1995;117:5614;
(b) Kato M, Kamigaito M, Sawamoto M, Higashimura T. Macromolecules 1995;28:1721–3.
[10] (a) Chiefari J, Chong YK, Ercole F, Krstina J, Jeffery J, Le TPT, et al. Macromolecules 1998;31:5559–62;
(b) Le TP, Moad G, Rizzardo E, Thang SH. PCT Int WO9801478; 1998.
[11] Solomon DH, Kambouris PA, Looney MG. PCT Int WO9831739; 1997.
[12] Solomon DH, Qiao GG, Abrol S. PCT Int WO99958588; 1999.
[13] Berge CT, Fryd M, Johnson JW, Moad G, Rizzardo E, Scopazzi C, et al. PCT Int WO0002939; 2000.
[14] Lord HT, Quinn JF, Angus SD, Whittaker MR, Stenzel MH, Davis TP. J Mater Chem 2003;13:2819–24.
[15] Barner-Kowollik C, Davis TP, Stenzel MH. Aust J Chem 2006;59:719–27.
[16] Wiltshire JT, Qiao GG. Macromolecules 2006;39:4282–5.
[17] Prochazka K, Baloch MK, Tuzar Z. Makromol Chem 1979;180:2521–3.
[18] O'Reilly RK, Hawker CJ, Wooley KL. Chem Soc Rev 2006;35:1068–83.
[19] Iijima M, Nagasaki Y, Okada T, Kato M, Kataoka K. Macromolecules 1999; 32:1140–6.
[20] Maskos M. Polymer 2006;47:1172–8.
[21] Erhardt R, Böker A, Zettl H, Kaya H, Pyckhout-Hintzen W, Krausch G, et al. Macromolecules 2001;34:1069–75.
[22] Walther A, Goldmann AS, Yelamanchili RS, Drechsler M, Schmalz H, Eisenberg A, et al. Macromolecules 2008;41:2254–360.
[23] Guo A, Liu GJ, Tao J. Macromolecules 1996;29:2487–93.
[24] (a) Gao H, Jones M-C, Chen J, Prud'homme RE, Leroux J-C. Chem Mater 2008;20:3063–7;
(b) Zhang J, Zhou Y, Zhu Z, Ge Z, Liu S. Macromolecules 2008;41:1444–54.
[25] (a) Walther A, Müller AHE. Soft Matter 2008;4:663–8;
(b) Walther A, Matussek K, Müller AHE. ACS Nano 2008;2:1167–78.
[26] Tao J, Stewart S, Liu G, Yang M. Macromolecules 1997;30:2738–45.
[27] Plamper FA, Becker H, Lanzendörfer M, Patel M, Wittemann A, Ballauff M, et al. Macromol Chem Phys 2005;206:1813–25.
[28] Furukawa T, Ishizu K. Macromolecules 2005;38:2911–7.
[29] Simms JA. Prog Org Coat 1993;22:367–77.
[30] Kennedy JP, Jacob S. Acc Chem Res 1998;31:835–41.
[31] Hadjichristidis N. J Polym Sci Part A Polym Chem 1999;37:857–71.
[32] (a) Matyjaszewski K. Polym Int 2003;52:1559–65;
(b) Kamigaito M, Ando T, Sawamoto M. Chem Record 2004;4:159–75.
[33] Hadjichristidis N, Pitsikalis M, Iatrou H. Polymers with star-related structures. In: Matyjeszewski K, Gnanou Y, Leibler L, editors. Macrmolecular engineering; precise synthesis, materials properties and applications. Weinheim: Wiley-VCH; 2007. p. 909–71 [chapter 6].
[34] Simms JA, Spinelli HJ. Macromolecular design of polymeric materials. In: Plastics engineering series, vol. 40. New York: Marcel Dekker; 1997 [chapter 22], p. 379–91.
[35] Hadjichristidis N, Pispas S, Pitsikalis M, Iatrou H, Vlahos C. Asymmetric star polymers: synthesis and properties. In: Advances in polymer chemistry, vol. 142. Berlin: Springer; 1999. p. 71–127.
[36] Grest GS, Fetters LT, Huang JS, Richter D. In: Prigogine I, Rice SA, editors. Advances in chemical physics, vol. 94. John Wiley & Sons; 1996. p. 67–163.
[37] Taton D. From stars to microgels. In: Matyjeszewski K, Gnanou Y, Leibler L, editors. Macromolecular engineering: precise synthesis, materials properties and applications. Weinheim: Wiley-VCH; 2007. p. 1007–56 [chapter 8].
[38] Gao H, Matyjaszewski K. Macromolecules 2008;41:1118–25.
[39] Baskaran D, Müller AHE. Prog Polym Sci 2007;32:173–219.
[40] Goethals EJ, Prez FD. Prog Polym Sci 2007;32:220–46.
[41] Moad G, Mayadunne RTA, Rizzardo E, Skidmore M, Thang SH. Macromol Symp 2003;192:1–12.
[42] Matyjaszewski K, Xia J. Chem Rev 2001;101:2921–90.
[43] (a) Xue L, Agarwal US, Zhang M, Staal BBP, Müller AHE, Bailly CME, et al. Macromolecules 2005;38:2093–100;
(b) Braunecker WA, Matyjaszewski K. Prog Polym Sci 2007;32:93–146.
[44] Terashima T, Ouchi M, Ando T, Kamigaito M, Sawamoto M. J Polym Sci Part A Polym Chem 2006;44:4966–80.
[45] Baek K-Y, Kamigaito M, Sawamoto M. Macromolecules 2001;34:215–21.
[46] Baek K-Y, Kamigaito M, Sawamoto M. Macromolecules 2001;34:7629–35.
[47] Baek K-Y, Kamigaito M, Sawamoto M. J Polym Sci Part A Polym Chem 2002;40:1972–82.
[48] Gao H, Ohno S, Matyjaszewski K. J Am Chem Soc 2006;128:15111–3.
[49] Helms B, Guillaudeu SJ, Xie Y, McMurdo M, Hawker CJ, Fréchet JMJ. Angew Chem Int Ed 2005;44:6384–7.
[50] Spiniello M, Blencowe A, Greg GG. J Polym Sci Part A Polym Chem 2008; 46:2422–32.
[51] Abrol A, Kambouris PA, Looney MG, Solomon DH. Macromol Rapid Commun 1997;18:755–60.
[52] Abrol S, Caulfield MJ, Qiao GG, Solomon DH. Polymer 2001;42:5987–91.
[53] Hawker CJ, Bosman AW, Harth E. Chem Rev 2001;101:3661–88.
[54] Benoit D, Chaplinski V, Braslau R, Hawker CJ. J Am Chem Soc 1999;121:3904.
[55] Xia J, Zhang X, Matyjaszewski K. Macromolecules 1999;32:4482–4.
[56] Moad G, Rizzardo E, Thang SH. Aust J Chem 2005;58:379–410.
[57] (a) Fröhlich MG, Vana P, Ziffere G. Macromol Theory Simul 2007;16:610–8;
(b) Fröhlich MG, Vana P, Ziffere G. J Chem Phys 2007;127:164906.
[58] Zheng G, Pan C. Polymer 2005;46:2802–10.
[59] Zhang L, Chen Y. Polymer 2006;47:5259–66.
[60] (a) Chaffey-Millar H, Stenzel MH, Davis TP, Coote ML, Barner-Kowollik C. Macromolecules 2006;39:6406–19;
(b) Barner L, Davis TP, Stenzel MH, Barner-Kowollik C. Macromol Rapid Commun 2007;28:539–59.

[61] Gurr P. The synthesis and characterisation of star-microgels by atom transfer radical polymerisation. Ph.D. thesis, The University of Melbourne; 2004.
[62] Zhang X, Xia J, Matyjaszewski K. Macromolecules 2000;33:2340–5.
[63] Baek K-Y, Kamigaito M, Sawamoto M. J Polym Sci Part A Polym Chem 2002;40:2245–55.
[64] Gao H, Matyjaszewski K. Macromolecules 2006;39:3154–60.
[65] Du J, Chen Y. J Polym Sci Part A Polym Chem 2004;42:2263–71.
[66] Chen J, Zhang H, Wang X, Liao X, Wang X. J Macromol Sci Pure Appl Chem 2006;43:269–77.
[67] Pasquale AJ, Long TE. J Polym Sci Part A Polym Chem 2001;39:216–23.
[68] Tsoukatos T, Pispas S, Hadjichristidis N. J Polym Sci Part A Polym Chem 2001;39:320–5.
[69] Bosman AW, Heumann A, Klaerner G, Benoit D, Fréchet JMJ, Hawker CJ. J Am Chem Soc 2001;123:6461–2.
[70] Amamoto Y, Higaki Y, Matsuda Y, Otsuka H, Takahara A. J Am Chem Soc 2007;129:13298–304.
[71] Zheng G, Pan C. Macromolecules 2006;39:95–102.
[72] Zheng Q, Zhen G, Pan C. Polym Int 2006;55:1114–23.
[73] Zheng G, Zheng Q, Pan C. Macromol Chem Phys 2006;207:216–23.
[74] Baek K-Y, Kamigaito M, Sawamoto M. J Polym Sci Part A Polym Chem 2002;40:633–41.
[75] Bosman AW, Vestberg R, Heumann AJ, Fréchet JMJ, Hawker CJ. J Am Chem Soc 2003;125:715–28.
[76] Fukukawa K-I, Rossin R, Hagooly A, Pressly ED, Hunt JN, Messmore BW, et al. Biomacromolecules 2008;9:1329–39.
[77] Zhang L, Katapodi K, Davis TP, Barner-Kowollik C, Stenzel MH. J Polym Sci Part A Polym Chem 2006;44:2177–94.
[78] Zhang P, Liu Q, Qing A, Shi J, Lu M. J Polym Sci Part A Polym Chem 2006; 44:3312–20.
[79] Hales M, Barner-Kowollik C, Davis TP, Stenzel M. Langmuir 2004;20: 10809–17.
[80] Wiltshire JT, Qiao GG. Macromolecules 2008;41:623–31.
[81] Du J, Chen Y. Macromolecules 2004;37:3588–94.
[82] Gao H, Tsarevsky NV, Matyjaszewski K. Macromolecules 2005;38: 5995–6004.
[83] Gao H, Matyjaszewski K. Macromolecules 2006;39:7216–23.
[84] Wiltshire JT, Qiao GG. Macromolecules 2006;39:9018–27.
[85] Gao H, Matyjaszewski K. J Am Chem Soc 2007;129:11828–34.
[86] Gao H, Matyjaszewski K. Macromolecules 2008;41:4250–7.
[87] (a) Ishizu K, Taiichi F, Ochi K. Architecture of star and hyperbranched polymers. In: Caruta BM, editor. Focus on polymeric materials research. Nova Science Publishers; 2006. p. 129–56 [chapter 6];
(b) Burchard W. Solution properties of branched macromolecules. In: Advances in polymer science, vol. 143. Berlin, Heidelberg: Springer-Verlag; 1999. p. 113–94.
[88] Qian Z, Minnikanti VS, Archer LA. J Polym Sci Part B Polym Phys 2008;46:1788–801.
[89] Santos A, Fantoni R, Giacometti A. Phys Rev E 2008;77:051206.
[90] Daoud M, Cotton JP. J Phys 1982;43:531–8.
[91] Goh TK, Coventry KD, Blencowe AB, Qiao GG. Polymer 2008;49:5095–104.
[92] Gurr PA, Qiao GG, Solomon DH, Harton SE, Spontak RJ. Macromolecules 2003;36:5650–4.
[93] Bouilhac C, Cloutet E, Cramail H, Deffieux A, Taton D. Macromol Rapid Commun 2005;26:1619–25.
[94] Narumi A, Yamane S, Miura Y, Kaga H, Satoh T, Kakuchi T. J Polym Sci Part A Polym Chem 2005;43:4373–81.
[95] Connal LA, Vestberg R, Hawker CJ, Qiao GG. Macromolecules 2007;40: 7855–63.
[96] Adkins CT, Harth E. Macromolecules 2008;41:3472–80.
[97] Gao H, Matyjaszewski K. Macromolecules 2007;40:399–401.
[98] Fukukawa K, Pressly E, Grupta N, Hawker CJ. Polym Prepr 2006;47: 466–7.
[99] Narumi A, Satoh T, Kaga H, Kakuchi T. Macromolecules 2002;35:699–705.
[100] Blencowe A, Kit GT, Best SP, Qiao GG. Polymer 2008;49:825–30.
[101] Terashima T, Kamigaito M, Baek K-Y, Ando T, Sawamoto M. J Am Chem Soc 2003;125:5288–9.
[102] Terashima T, Ouchi M, Ando T, Kamigaito M, Sawamoto M. Macromolecules 2007;40:3581–8.
[103] Baek K-Y, Kamigaito M, Sawamoto M. Macromolecules 2002;35:1493–8.
[104] Isonaga M, Satoh K, Kamigaito M, Okamoto Y. Polym Prepr 2005; 46:401–2.
[105] Chi Y, Scroggins ST, Fréchet JMJ. J Am Chem Soc 2008;130:6322–3.
[106] Wei B, Gurr PA, Genzer J, Qiao GG, Solomon DH, Spontak RJ. Macromolecules 2004;37:7857–60.
[107] Wei B, Gurr PA, Gozen AO, Blencowe A, Solomon DH, Qiao GG, et al. Nano Lett 2008;8:3010–6.
[108] Connal LA, Gurr PA, Qiao GG, Solomon DH. J Mater Chem 2005;15:1286–92.
[109] Connal LA, Vestberg R, Gurr PA, Hawker CJ, Qiao GG. Langmuir 2008;24: 556–62.
[110] Connal LA. Aust J Chem 2007;60:794.
[111] Connal LA, Qiao GG. Adv Mater 2006;18:3024–8.
[112] Connal LA, Qiao GG. Soft Matter 2007;3:837–9.
[113] Ho AK, Lin L, Gurr PA, Mills MF, Qiao GG. Polymer 2005;46:6727–35.
[114] (a) Grest GS, Fetters LJ, Huang JS, Richter D. Adv Chem Phys 1996;XCIV: 67–164;
(b) Vlassopoulos D, Fytas G, Pakula T, Roovers J. J Phys Condens Matter 2001;13:R855–76;
(c) Vlassopoulos D, Fytas G, Pispas S, Hadjichristidis N. Physica B 2001;296: 184–9.
[115] Goh TK, Sulistio AP, Blencowe A, Johnson JW, Qiao GG. Macromolecules 2007;40:7819–26.
[116] Seidlits S, Peppas NA. Star polymers and dendrimers in nanotechnology and drug delivery. In: Peppas NA, editor. Nanotechnology in therapeutics. Taylor & Francis; 2007. p. 317–48 [chapter 13].
[117] Duncan R. Nat Rev 2003;2:347–60.
[118] Peppas NA, Nagai T, Miyajima M. Pharm Technol Jpn 1994;10:611–7.
[119] (a) Liu M, Kono K, Fréchet JMJ. J Controlled Release 2000;65:121–31;
(b) Kojima C, Kono K, Maruyama K, Takagishi T. Bioconjugate Chem 2000;11:910–7.
[120] Wiltshire JT, Qiao GG. Aust J Chem 2007;60:699–705.
[121] Chan Y, Wong T, Byrne F, Kavallaris M, Bulmus V. Biomacromolecules 2008;9:1826–36.
[122] Connal LA, Li Q, Quinn JF, Tjipto E, Caruso F, Qiao GG. Macromolecules 2008;41:2620–6.
[123] Wolterink JK, van Male JM, Stuart AC, Koopal LK, Zhulina EB, Borisov OV. Macromolecules 2002;35:9176–90.
[124] Furukawa T, Uchida S, Ishizu K. J Appl Polym Sci 2007;105:1543–50.
[125] Ge Z, Xu J, Wu D, Narain R, Liu S. Macromol Chem Phys 2008; 209:754–63.
[126] Weaver JVM, Williams RT, Royles BJL, Findlay PH, Cooper AI, Rannard SP. Soft Matter 2008;4:985–92.
[127] Shusharina NP, Rubinstein M. Macromolecules 2008;41:203–17.

Anton Blencowe graduated with a First Class Honours MChem degree in Chemistry from the University of Reading in July 2002. During the final year studies of his degree he conducted a research project in the Hayes Research Group focusing upon the synthesis of hyperbranched diacetylene polyesters. He commenced postgraduate studies sponsored by the DuPont Fellows Forum at the University of Reading in 2002 under the guidance of Dr. Wayne Hayes. After completion of his Ph.D. entitled "*The Development of Polymerisation and Surface Modification Techniques using Diazirines as Carbene Precursors*" in 2006 he took up a Research Fellow position in the Polymer Science Group at The University of Melbourne. Since his appointment he has been awarded several Early Career Researcher Grants for the development of advanced materials and works on projects ranging from the development of functional polymers for tissue engineering and polymer therapeutics, to polymers for metal extraction and coatings technologies. His research interests include, amongst other things: star polymer synthesis, properties and applications; the development of novel macromolecular architectures and polymerisation methodologies; biomacromolecular scaffolds.

Jing Fung Tan graduated with a B.Eng (Hons) in Chemical Engineering from University of Melbourne in 2006. During his undergraduate studies he was awarded the Melbourne Abroad Scholarship in 2004 for an exchange program to Imperial College London. Upon graduation, he was awarded an Australian Postgraduate Award (Industry) funded by DuPont and commenced his Ph.D. studies in the Polymer Science Group under the guidance of Associate Professor Greg Qiao in the same year. He was also the 2006 President of the Postgraduate Association of Chemical Engineers at The University of Melbourne. His research focuses on the synthesis of novel polymeric architectures via controlled and conventional radical polymerisation techniques.

Tor Kit Goh graduated with a Bachelor of Engineering (Chemical) (Hons) from the University of Melbourne in December 2004. He subsequently joined the Polymer Science Group and is currently conducting research on star polymers for advanced coatings applications with A/Prof. Greg Qiao as his mentor. His postgraduate research is funded by an ARC-DuPont Linkage Grant – Australian Postgraduate Award (Industry) and he was recently awarded the 2008 Endeavour Research Fellowship, which supported a 6-month research project on stereospecific living radical polymerisation with Prof. Masami Kamigaito of Nagoya University. His research interests include polymer chemistry, synthesis of macromolecular architectures and polymer rheology.

Greg G. Qiao received his B.Eng. in Polymer Engineering from the East China University in 1982. He completed his synthetic organic chemistry based Ph.D. under the supervision of Professor Curt Wentrup at the University of Queensland in 1996. Subsequently, he worked as a Postdoctoral Fellow with Professor David Solomon at the University of Melbourne, where he was introduced to the field of synthetic polymers. Since 2000 he has been the leader of the Polymer Science Group at the University of Melbourne. He is now a Reader in the Department of Chemical and Biomolecular Engineering and an Assistant Dean (Research) in the Melbourne School of Engineering. He is also a Fellow of the Royal Australian Chemical Institute (FRACI). His major current research interests are in the synthesis of novel macromolecular architectures by controlled polymerisation techniques, polymeric membranes for gas separations, biomacromolecular scaffolds for soft tissue engineering and functional polymers for industrial applications.